

RESEARCH ARTICLE

Representation of the Indian Ocean Walker circulation in climate models and links to Kenyan rainfall

James A. King  | Richard Washington | Sebastian Engelstaedter

School of Geography and the
Environment, University of Oxford,
Oxford, UK

Correspondence

James A. King, School of Geography and
the Environment, University of Oxford,
Oxford, UK.

Email: james.king@linacre.ox.ac.uk

Funding information

Natural Environment Research Council,
Grant/Award Number: NE/L002621/1

Abstract

Reliable climate change projections over East Africa are vital because of regional vulnerability to precipitation changes. However, global climate models from Coupled Model Intercomparison Project Phase 5 (CMIP5) display significant biases in their representation of key East African rainfall seasons, which call into question the reliability of projected climate change. We investigate the links between models' representation of rainfall over Kenya during the long and short rains and the proximate Walker circulation. There is a strong correlation in the short rains between model biases in Kenyan rainfall and in the mid-to-upper tropospheric vertical velocity associated with this circulation. The overturning Indian Ocean Walker cell at the equator is absent in 5/25 models during the short rains – these models exhibit wet biases. In the long rains, dry biased models overestimate the strength of the descending limb of the circulation over East Africa. Omega biases over the Congo Basin are linked to broader Walker circulation biases. During the long rains, models overestimate equatorial descent more generally across the Western Hemisphere Tropics (0°E–200°E). A significant correlation is obtained across the model ensemble between model rainfall over Kenya and Western Hemisphere equatorial ascent during November. Atmosphere-only models display some improvements over coupled models, but biases of a similar magnitude remain. We therefore propose Indian Ocean Walker circulation errors as a key source of bias in CMIP5 East African rainfall. The results add to recent work on CMIP5 biases in this region, demonstrating that the Indian Ocean Walker circulation should be a focus for future model improvement and a consideration when assessing the reliability of climate projections over East Africa. Further work is needed on the causes of Walker circulation biases (in particular the role of SST), and on understanding the impact of Walker circulation biases on modelled tropical rainfall elsewhere in the world.

KEYWORDS

climate, East Africa, general circulation model experiments, rainfall, Tropics, Walker circulation

This is an open access article under the terms of the Creative Commons Attribution License, which permits use, distribution and reproduction in any medium, provided the original work is properly cited.

© 2020 The Authors. International Journal of Climatology published by John Wiley & Sons Ltd on behalf of the Royal Meteorological Society.

1 | INTRODUCTION

Climate models are our primary tool for projecting the global climate system's response to warming brought about by anthropogenic greenhouse gas emissions. They are used to formulate policy on scales from the global to the local, but often exhibit substantial biases in vital output fields such as precipitation (Li and Xie, 2014; James *et al.*, 2015; 2018; Rowell *et al.*, 2015; Tierney *et al.*, 2015; Ongoma *et al.*, 2017). In some regions of the world, models display sizeable systematic biases relative to observations – errors which, having a shared direction, may be indicative of a common underlying dynamical problem (Sanderson and Knutti, 2012). It is therefore important to understand the underlying physical processes operating within models with respect to biases, so that these biases can be both foci for targeted model improvement (James *et al.*, 2015; 2018; Collins *et al.*, 2018) and can be taken into account when assessing the reliability of projections derived from a specific model or model ensemble (McSweeney *et al.*, 2015). Global climate models are run at spatial resolutions that make it difficult to replicate the complexity of the circulation responsible for specific characteristics of regional circulations. The approach whereby climate model performance is evaluated based on dynamical processes is therefore of particular use in climate projections on smaller spatial scales useful to policy-makers (Collins *et al.*, 2018), and is more revealing than simply relying on a comparison between model output and a reference dataset (James *et al.*, 2015), especially in regions such as the tropics where observational data may be sparse or of poor quality (Washington *et al.*, 2013; Gebrechorkos *et al.*, 2018). Therefore, studying model dynamics in such regions can have useful impacts on both the modelling and climate adaptation communities.

Models participating in the Coupled Model Intercomparison Project Phase 5 (CMIP5; Taylor *et al.*, 2012) exhibit systematic biases in their representation of historical rainfall over East Africa (Yang *et al.*, 2014; Tierney *et al.*, 2015). The models tend to underestimate rainfall in the long rains season (March–April–May), some by over half, and to overestimate it in the short rains season (October–November–December), some by over 100%. In historical coupled simulations, the magnitude of the model ensemble range (i.e., the difference between the wettest and driest models) is greater than the observed monthly mean rainfall in all rainy season months other than April (Tierney *et al.*, 2015).

An understanding of model rainfall biases is crucial to climate change adaptation planning in East Africa (Collier *et al.*, 2008; Shongwe *et al.*, 2011; Uhe *et al.*, 2018). Around 75% of the working population are involved in

rain-fed agriculture (Lyon, 2014), and hydroelectricity provides the majority of the region's energy; rainfall is thus closely linked to development (Funk *et al.*, 2008; Borgomeo *et al.*, 2018). East Africa has recently experienced a series of severe droughts, for example in 1983–1984 and 2010–2011 (Lyon, 2014), with drought conditions prevailing since around 2008 (Nicholson, 2016a). Around 17.5 million people are at risk from food shortages in Ethiopia, Somalia, and Kenya (Williams and Funk, 2011) and links have been suggested between drought and conflict in Somalia (Thalheimer and Webersik, 2020). Uncertain rainfall projections raise significant dilemmas (Washington *et al.*, 2006; Giannini *et al.*, 2018). For instance, should countries invest in more irrigation infrastructure and hydroelectric power, given projected rainfall increases (Kaunda *et al.*, 2012)? Or, rather, should they focus on reducing the impacts of drought events, given the climatic trends of the last 30–40 years? A first step towards addressing these questions is an understanding of the causes behind models' rainfall biases. Elsewhere in Africa, model rainfall bias has been shown to condition the nature of projected climate change (Munday and Washington, 2018).

The seasonal cycle of rainfall in East Africa is associated with the northward/southward movement of the tropical rain belt, although the complexity of the local topography and rainfall dynamics limits the explanatory power of this feature (Nicholson, 2018). Important fundamental influences on East African rainfall include moisture flux from the Indian Ocean (Viste and Sorteberg, 2013; Yang *et al.*, 2015b), moist static energy profiles (Yang *et al.*, 2015b), and topography (Slingo *et al.*, 2005; Hession and Moore, 2011; Naiman *et al.*, 2017). Dynamically the rainfall is modulated on intraseasonal to interannual timescales by the Madden-Julian Oscillation (Berhane and Zaitchik, 2014; Zaitchik, 2017), Indian Ocean SST, and the Quasi-Biennial Oscillation (Vellinga and Milton, 2018). The understudied low-level jet in the Turkana Channel may also have a role in controlling regional aridity and rainfall variability (Nicholson, 2016b; Hartman, 2018; MacLeod, 2019).

Efforts to understand the nature of future climate change have put a premium on circulation over thermodynamics in the tropical atmosphere (Chadwick *et al.*, 2013). On a global scale, the wider multi-cell Walker circulation is associated with the El Niño Southern Oscillation (ENSO), and while the strength of the teleconnection between East African rainfall and ENSO, primarily observed during the short rains, has varied throughout the observational record (Nicholson, 2015), the Walker circulation may act as a mechanism by which the ENSO signal (and Pacific SST warming more

generally) is transmitted to East Africa via modification of vertical velocity and moisture transport (Black, 2005; Hoell *et al.*, 2014; Lyon, 2014).

Models tend to exhibit positive IOD biases in boreal autumn and winter (Cai and Cowan, 2013), but attribution of recent East African spring drying to the IOD is limited because the IOD is generally neutral in this season. Furthermore, the tendency of models to project increasing spring rainfall under future forcing scenarios, in direct contrast to the recent observed drying trend, has been termed the 'East African Climate Paradox' (Rowell *et al.*, 2015; Wainwright *et al.*, 2019). While the 'paradox' refers to the long rains, the majority of the models' projections of wetting occur during the short rains in response to projected Walker circulation weakening (Kociuba and Power, 2015; Tierney *et al.*, 2015; Endris *et al.*, 2018). This is in opposition to recent observations, leading the models' representation of the Walker circulation to become a significant source of uncertainty in future projections (Tierney *et al.*, 2015; Giannini *et al.*, 2018).

The link between the Walker circulation and East African rainfall in observations has been well established (e.g., Black *et al.*, 2003; Behera *et al.*, 2005; Liebmann *et al.*, 2014; 2017; Vigaud *et al.*, 2017), particularly for the short rains where there is a strong correlation between surface equatorial westerlies and rainfall (Mutai *et al.*, 2012). These westerlies, which form part of the overturning Walker cell in the Indian Ocean, are in turn closely correlated with the zonal SST gradient in the Indian Ocean. This is most pronounced during boreal winter when the Indian Ocean Dipole (IOD) is most active (Black, 2005). The Pacific component of the Walker circulation has been observed to be strengthening on decadal timescales since the 1950s (L'Heureux *et al.*, 2013), coincident with a decadal drying signal over East Africa during the long rains (Rowell *et al.*, 2015). A dynamic link between the two has been suggested; SST warming in the eastern Indian Ocean (a negative IOD) has led to increased convection/precipitation in the east of the basin (Liebmann *et al.*, 2017), resulting in easterly movement of air aloft which suppresses convection over East Africa (Williams and Funk, 2011; Liebmann *et al.*, 2017). Recent work has linked model rainfall biases in East Africa to erroneous low-level zonal winds over the equatorial Indian Ocean (Hirons and Turner, 2018), which are part of the overturning circulation. The Walker circulation has also been found to be poorly represented over Madagascar, with an overly simplified connection between Indian Ocean subsidence and Southern African convection (Munday and Washington, 2018). Given that SST warming in the Indian and Pacific oceans is likely to be anthropogenic, whereas ENSO is fundamentally a

natural mode of variability modified by warming, it is likely that both anthropogenic and natural forcings need to be considered to explain the recent drying trend – however, model biases frustrate such attribution (Hoell *et al.*, 2017). In addition, work on the Walker circulation tends to focus on the zonal winds and/or the ascending component, whereas both ascending and descending components interact to produce observed rainfall (Li *et al.*, 2015). Here, we add to this analysis by presenting an assessment of how models' circulation biases affect their rainfall biases. We aim to address the following questions:

1. What is the relationship between the reanalysis vertical components of the Indian Ocean Walker circulation and observed Kenyan rainfall?
2. How is this relationship represented in CMIP5 models?
3. How are the CMIP5 rainfall biases in the East African region associated with their simulations of the Walker circulation?

The layout of the rest of the article is as follows: Section 2 introduces the datasets used. Section 3 reviews the rainfall climatology of Kenya and examines the Walker circulation/rainfall relationship using gridded rainfall and reanalysis data. Section 4 analyses the representation of the Walker circulation in CMIP5 models and its links to Kenyan rainfall. Section 5 summarizes the article in the context of future climate projections, and provides a conclusion.

2 | DATA

Rainfall data used in this study were obtained from version 2 of the Climate Hazards Group Infrared Precipitation with Stations dataset (CHIRPSv2.0; Funk *et al.*, 2015). This is a high-resolution (0.05°) gridded dataset which combines observed rainfall from raingauges with remotely sensed infrared measurements of cold cloud duration. It has performed well in assessments of precipitation datasets over East Africa relative to station data, and has been suggested to be the best available satellite estimate of rainfall over eastern equatorial Africa (Kimani *et al.*, 2017; Gebrechorkos *et al.*, 2018). Given the lack of direct observations of the upper troposphere, reanalysis data were used as the reference climatology for the Walker circulation. Reanalysis products differ slightly in their representations of the tropospheric circulation over equatorial Africa (Washington *et al.*, 2013; Maidment *et al.*, 2015). While the difficulty of obtaining direct observations of tropospheric vertical motion over

TABLE 1 CMIP5 models used in this study. Expansions of acronyms are available online at <http://www.ametsoc.org/PubsAcronymList>. Asterisks denote models used in AMIP ensemble.

Model name	Modelling group	Mean March Kenya rainfall (mm·day ⁻¹)	Mean November Kenya rainfall (mm·day ⁻¹)
ACCESS1-3*	Commonwealth Scientific and Industrial Research Organization and Bureau of Meteorology (Australia)	0.72018468	5.39158201
BCC-CSM1-1-M*	Beijing Climate Centre, China Meteorological Administration	3.12062645	4.77377367
BNU-ESM*	College of Global Change and Earth System Science, Beijing Normal University	0.50848675	2.30800176
CanESM2	Canadian Centre for Modelling and Analysis	2.20307994	3.82551479
CanAM4* (atmosphere only)	Canadian Centre for Modelling and Analysis	3.519263	4.191565
CCSM4*	National Center for Atmospheric Research (USA)	1.12436569	4.88698149
CESM1-CAM5*	National Science Foundation, Department of Energy, National Center for Atmospheric Research (USA)	0.88511753	4.35356998
CMCC-CM*	Centro Euro-Mediterraneo per I Cambiamenti Climatici (Italy)	1.52150857	3.66852021
CNRM-CM5*	Centre National de Recherches Météorologiques (France)	1.19458139	3.20929885
CSIRO-Mk3-6-0*	Commonwealth Scientific and Industrial Research Organisation in collaboration with the Queensland Climate Change Centre of Excellence (Australia)	1.85005295	3.11245489
EC-EARTH	EC-EARTH consortium (Europe)	1.29948533	3.00232744
FGOALS-g2*	LASG, Institute of Atmospheric Physics, Chinese Academy of Sciences; and CESS, Tsinghua University	1.54839027	4.2387495
FIO-ESM	The First Institute of Oceanography, SOA (China)	1.97875655	2.83555794
GFDL-CM3*	Geophysical Fluid Dynamics Laboratory (USA)	0.35625046	4.54361105
GISS-E2-R*	Goddard Institute for Space Studies (USA)	2.65551329	4.94359398
HadGEM2-A* (atmosphere only)	Met Office Hadley Centre (UK)	2.047307	3.890381
HadGEM2-AO	Met Office Hadley Centre (UK)	0.99927062	3.21843314
INMCM4*	Institute for Numerical Mathematics (Russia)	3.36340737	5.58793449
IPSL-CM5A-LR*	L'Institut Pierre-Simon Laplace (France)	0.67848229	1.46617961
IPSL-CM5A-MR*	L'Institut Pierre-Simon Laplace (France)	1.60588074	1.69666374

(Continues)

TABLE 1 (Continued)

Model name	Modelling group	Mean March Kenya rainfall (mm day ⁻¹)	Mean November Kenya rainfall (mm day ⁻¹)
IPSL-CM5B-LR*	L'Institut Pierre-Simon Laplace (France)	0.37739533	3.11946
MIROC5*	National Institute for Environmental Studies (Japan), Atmosphere and Ocean Research Institute (University of Tokyo), Japan Agency for Marine-Earth Science and Technology	2.63725114	2.90290928
MIROC-ESM-CHEM	National Institute for Environmental Studies (Japan), Atmosphere and Ocean Research Institute (University of Tokyo), Japan Agency for Marine-Earth Science and Technology	1.26737058	3.3539691
MPI-ESM-LR*	Max Planck Institute for Meteorology (Germany)	0.75810111	1.71675229
MPI-ESM-MR*	Max Planck Institute for Meteorology (Germany)	0.88501096	2.56478405
MRI-AGCM3-2H* (atmosphere only)	Meteorological Research Institute (Japan)	2.567191	3.473036
MRI-CGCM3	Meteorological Research Institute (Japan)	0.52001166	4.85260153
NorESM1-M*	Norwegian Climate Centre	1.74336731	5.244816

the oceans precludes direct validation studies for the time being, version 2 of the Modern-Era Retrospective Analysis for Research and Applications (MERRA-2) reanalysis (Gelaro *et al.*, 2017) has been suggested to be the most realistic of those currently available at representing tropospheric wind fields over equatorial Africa when compared to quality-controlled observations from radiosondes (Hua *et al.*, 2019). Given that such winds are part of the overturning cells upon which this article is focussed, MERRA-2 data has been used. ERA-Interim and NCEP2 data produced similar results (not shown).

The climate model data used are from CMIP5 (Taylor *et al.*, 2012). A subset of 25 GCMs was selected based upon the availability of vertical velocity and wind fields from the historical coupled runs, and forcing experiments with the RCP8.5 scenario (which is the closest to observed recent CO₂ concentration increases [Sanford *et al.*, 2014]) for use in future work (Table 1). The first ensemble member for each model was used over the period 1975–2005. Initial analysis using the first three ensemble members for two randomly selected models (ACCESS1-3 and MPI-ESM-LR) indicated that the results were not sensitive to the ensemble member selected – no statistically significant differences were found between the ensemble members for the correlations between monthly mean precipitation and 400 hPa vertical velocity over Kenya. The individual models varied in resolution from 0.5625° to 7.84°. Consequently, where model composites were calculated, the data were first regridded onto a common 1° x 1° grid using a nearest neighbour interpolation algorithm. A subset of 22 atmosphere-only models (AMIP) was selected from the CMIP5 ensemble, which are denoted with asterisks in Table 1. Analysis involving wind field computations using spherical harmonic functions (e.g., velocity potential) was performed using the Windspharm library (Dawson, 2016).

3 | OBSERVATIONS AND REANALYSIS

The vertical motion associated with the Walker circulation acts as a large-scale control on rainfall over Kenya during the short rains (Mutai *et al.*, 2012). It has been suggested as a mechanism for recent drying trends in the long rains (Williams and Funk, 2011), and many CMIP5 models exhibit mean-state biases in the low-level zonal winds which are associated with the circulation (Hirons and Turner, 2018). We explore the possibility that rainfall biases in CMIP5 models are linked to the models' representation of vertical motion in both the ascending and descending limbs of the Indian Ocean Walker circulation.

Here, we briefly review the climatological Walker circulation and its links to the observed rainfall climatology within the two main Kenyan rainy seasons.

Rainfall in the Greater Horn of Africa (GHA) region generally displays either a unimodal or bimodal regime. The Ethiopian Highlands region has a unimodal rainfall climatology with a rainy season extending from July to September (Dunning *et al.*, 2016), although there is complex seasonality in sub-regions (Diro *et al.*, 2011). Areas further south, including Kenya, have a bimodal rainfall climatology, with a 'long rains' season from March to May and a 'short rains' which is considered by some to extend from October to December (Yang *et al.*, 2015a) but by others to only include October and November (e.g., Nicholson, 2017). Figure 1 illustrates the spatial distribution of rainfall in each month of these two rainy seasons. For Kenya, rainfall maxima in excess of $250 \text{ mm-month}^{-1}$ are located in the central highlands around Mt. Kenya in April and November, as well as along the eastern edge of Lake Victoria in April and along the coast in May. North-west Kenya, around Lake Turkana, is consistently dry with less than $100 \text{ mm-month}^{-1}$ of rainfall in each month of the rainy seasons. Averaged across the Kenya domain (box in

Figure 1), the wettest long rains month is April (4.22 mm-day^{-1}) and the wettest short rains month is November (3.06 mm-day^{-1}).

The climatological structure of the vertical velocity (ω) component of the Indian Ocean Walker circulation in MERRA2 reanalysis can be seen in Figures 2, 3, and 4. The core ascending region over the Maritime Continent is strongest in April during the long rains (-0.065 Pa-s^{-1}) and November during the short rains (-0.094 Pa-s^{-1}) (Figure 2). In March, the upper-tropospheric descent over Kenya is 10° more longitudinally extensive than in April and 20° more extensive than in May. The region of ascent over the Indian Ocean is more extensive in May; there are also clear differences in the strength of descent between the months. March (0.027 Pa-s^{-1}) and May (0.021 Pa-s^{-1}) have stronger descent over Kenya than April (0.013 Pa-s^{-1}). October (0.029 Pa-s^{-1}) and December (0.027 Pa-s^{-1}) have stronger descent than November (0.024 Pa-s^{-1}) (Figure 2). Months within the rainy seasons are characterized by ascending air throughout the troposphere extending westward as far as 50°E (December) from the Maritime Continent across the Equatorial Indian Ocean. We

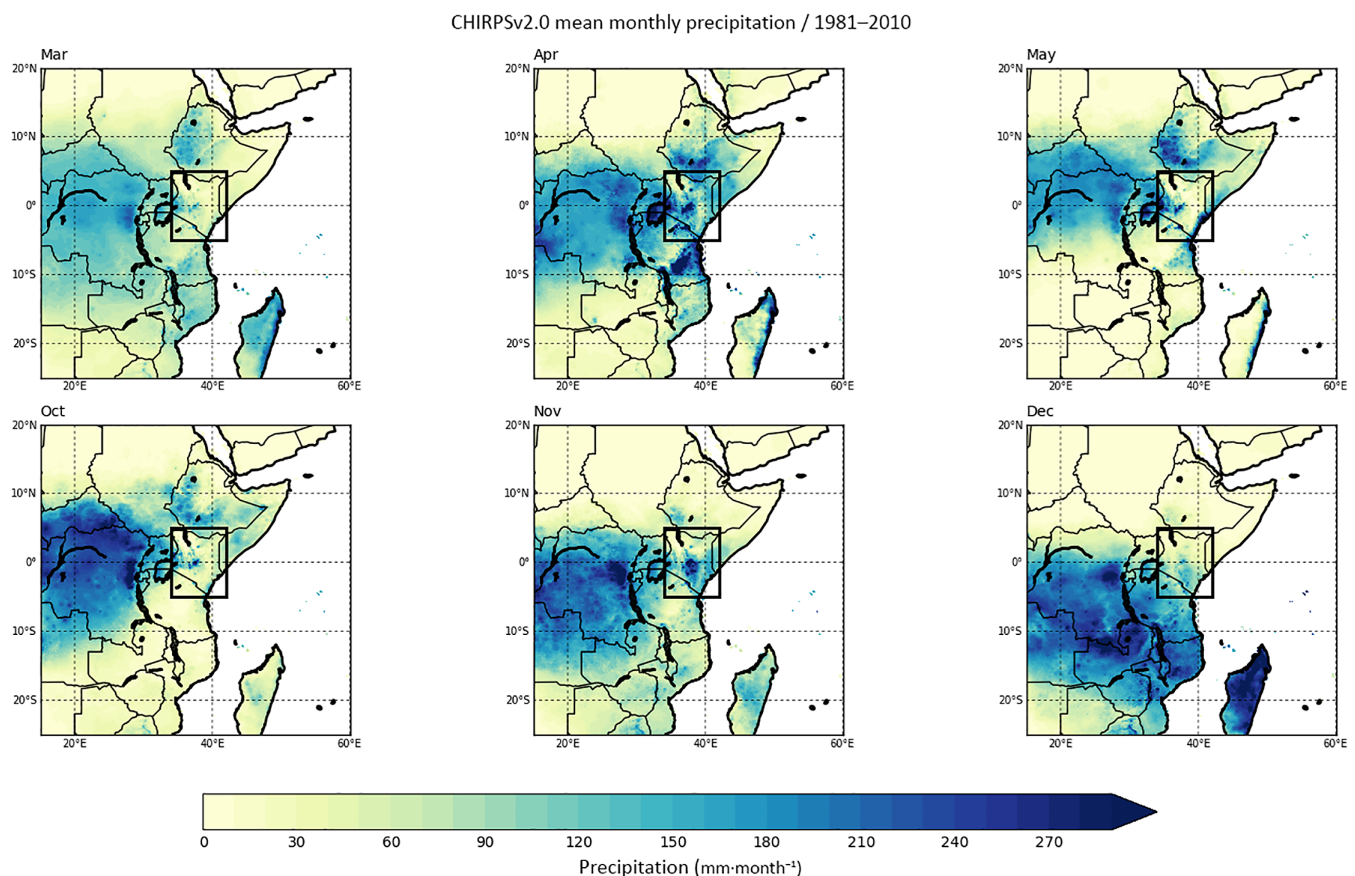


FIGURE 1 CHIRPS v2.0 rainfall climatology for East Africa averaged for each month in the period 1981–2010. The black box shows the area over which Kenya rainfall is averaged

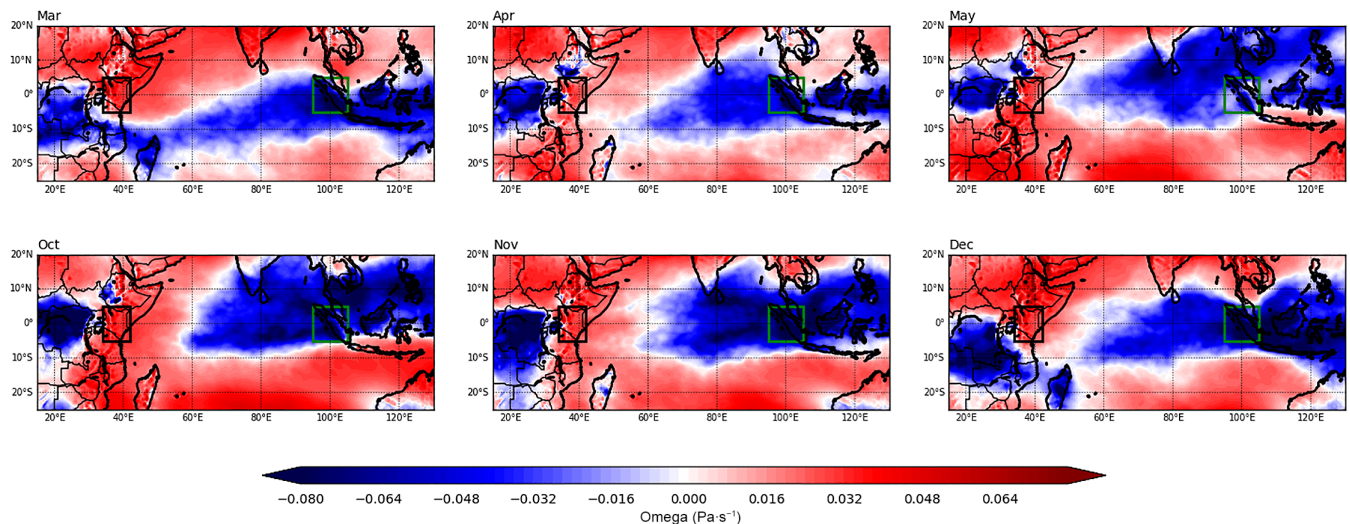


FIGURE 2 MERRA-2 omega at 400 hPa for each rainy season month, averaged over 1980–2008. The black box indicates the area used for averaging fields over Kenya, and the green box indicates that used for averaging fields over the Eastern Indian Ocean

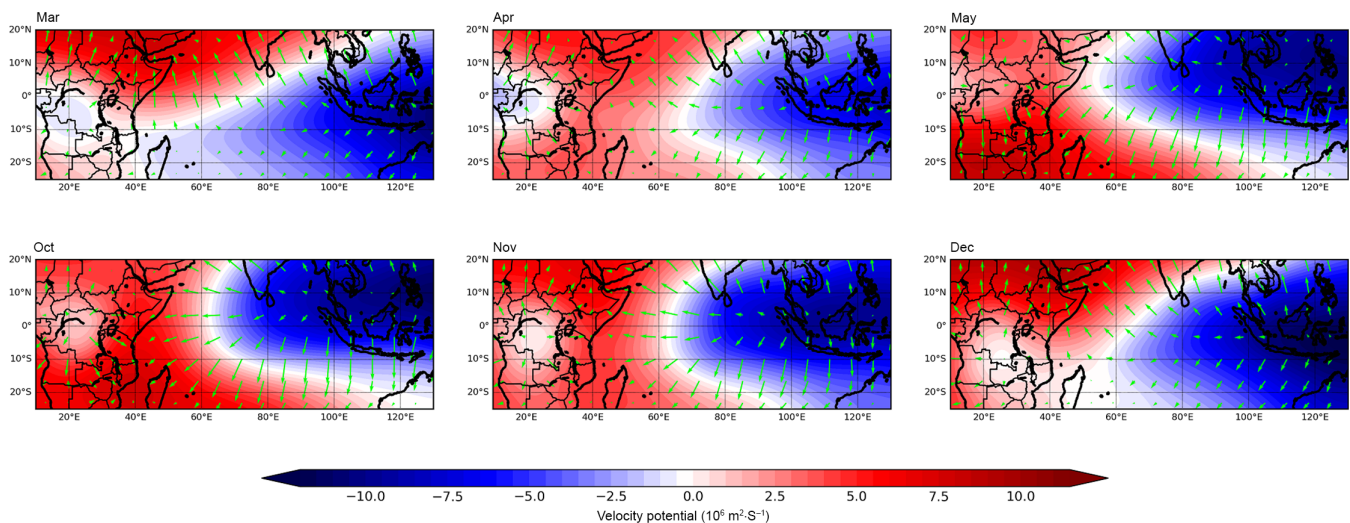


FIGURE 3 MERRA-2 velocity potential (filled contours) and divergent wind vectors (arrows) at 200 hPa for each rainy season month, averaged over 1980–2008

extend this analysis of vertical motion to the 200 hPa velocity potential field and its associated divergent wind, which is frequently used to diagnose overturning circulations in the Tropics by linking the lifting of the 200 hPa geopotential to patterns of convergence and divergence in the wind field. (Tanaka *et al.*, 2004; Schwendike *et al.*, 2014; Hart *et al.*, 2018). Figure 3 indicates that a zonal gradient in large-scale atmospheric vertical motion is present across the equatorial Indian Ocean in MAM and OND, and also indicates upper-level convergence over Kenya associated with

both the Maritime Continent and Congo Basin regions of ascent.

The descending limb of the circulation overlies Kenya (34°E–42°E), extending down to around 700 hPa over the land, below which there is ascent (Figure 4). The effects of the region's complex topography can be seen near to the surface, with alternating bands of ascent and descent suggestive of localized overturning circulations in the East African Highlands around Lake Victoria (Figure 4). The strength and extent of the descending limb acts as an upper limit on deep convection over Kenya to a varying

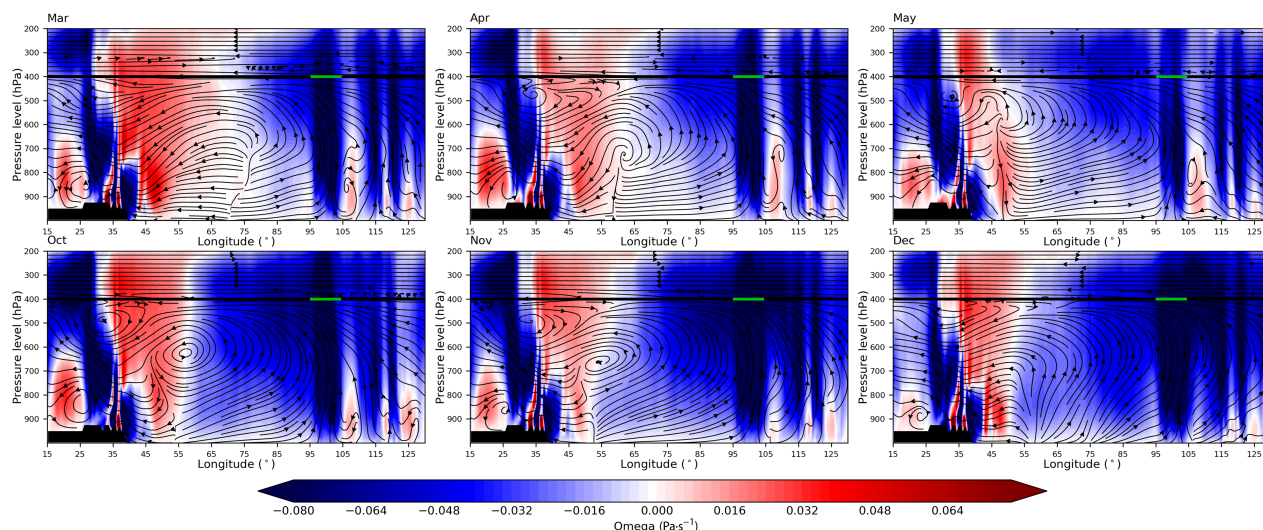


FIGURE 4 Longitude-height plots of MERRA-2 reanalysis climatology for MAM (top row) and OND (bottom row), 1980–2008, 15°E–130°E, averaged over 5°N–5°S. Shading is vertical velocity ($\text{Pa}\cdot\text{s}^{-1}$) with red indicating negative (upward) motion and blue indicating positive (downward) motion. Streamlines are the resultant vectors of u and $w \times 10^4$. The black line indicates the 400 hPa level. The green line indicates the box used for averaging over the ascending limb of the Walker circulation

TABLE 2 Pearson product moment correlation coefficients between CHIRPS v2.0 rainfall and MERRA-2 400 hPa omega, averaged over Kenya ($N = 24$, $R_{\text{crit}} = 0.388$)

March	April	May	October	November	December
$R = -0.769$	$R = -0.720$	$R = -0.573$	$R = -0.260$	$R = -0.847$	$R = -0.797$
$p = 7.104\text{E}-06$	$p = 9.37\text{E}-06$	$p = 0.00274$	$p = 0.209$	$p = 9.073\text{E}-08$	$p = 1.846\text{E}-06$

degree depending on the month. The wettest months in the two rainy seasons (April and November) correspond to the periods when descent over Kenya is weaker and ascent over the Indian Ocean is stronger. This suggests that the Walker circulation strength could explain why April and November are the wettest months within the Kenyan rainy seasons.

The streamlines in Figure 4 indicate the presence of an overturning circulation which is more pronounced during the less wet short rains, particularly in October/November, but is also active during the long rains. The circulation is characterized by lower-tropospheric westerlies and mid-to-upper-tropospheric easterlies over the eastern equatorial Indian Ocean.

Statistically significant negative correlations ($p < 0.05$) were obtained between Kenya rainfall and 400 hPa omega averaged over Kenya for all rainy season months in the period 1981–2005 (Table 2), except October. The correlations were strongest in March during the long rains, and in November during the short rains. A significant correlation for October ($p < 0.1$) was obtained after the anomalously wet October of 1997 was removed. This suggests an

important role for omega in controlling climatological rainfall over Kenya during the rainy seasons. The following analysis links this to the descending limb of the Indian Ocean Walker circulation.

Figure 5 reveals the dominant structure of the Indian Ocean Walker circulation associated with Kenyan rainfall. There is a strong negative correlation between observed rainfall over Kenya and reanalysis omega at 400 hPa, both over the country itself and over the western Indian Ocean throughout the rainy seasons. This refers to enhanced Kenyan rainfall when the climatological descent over this region is weakened. An exception is October, where the correlation over Kenya itself is positive – this explains the lack of a significant correlation in Table 2 prior to the removal of data from 1997. There is a significant positive correlation in the eastern Indian Ocean which is most pronounced during the short rains; this refers to higher rainfall over Kenya when the ascending limb of the Indian Ocean Walker circulation over the western Indian Ocean is weaker. Additionally, we calculated the interannual Pearson product moment correlation coefficient (for MERRA2 monthly data) between the

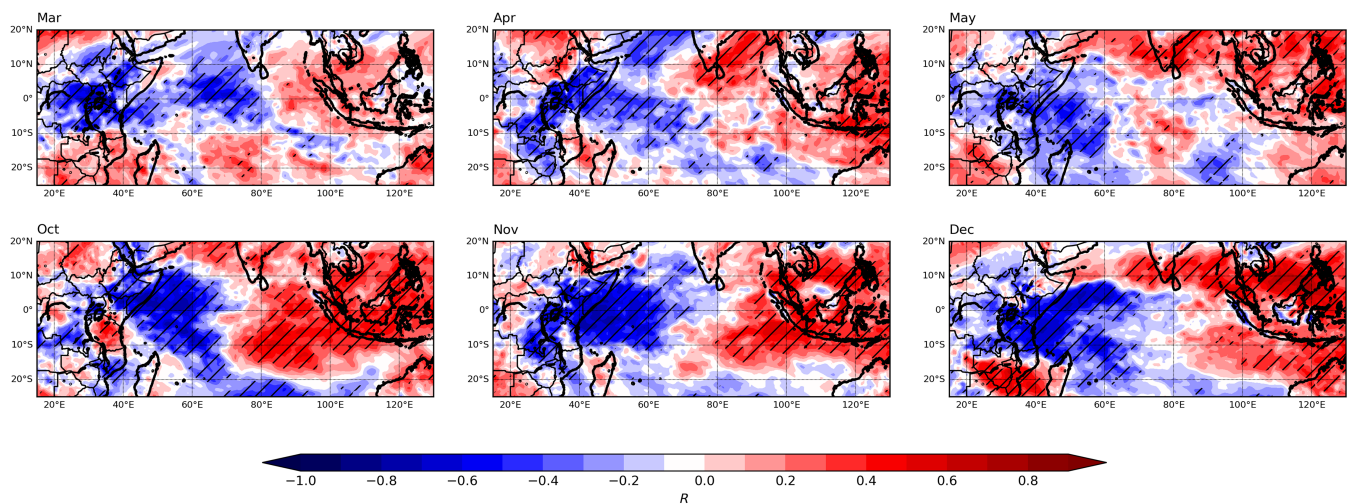


FIGURE 5 Pearson product moment correlation coefficient between CHIRPS v2.0 rainfall averaged over Kenya and MERRA-2 400 hPa omega for 1980–2008. Hatching indicates significance at $p < 0.1$

400 hPa omega over Kenya and the equatorial zonal winds at 850 hPa using the box defined in Figure 6a of Hirons and Turner (2018) (50°E–100°E, 5°N–5°S). For OND, we obtained a value of $r = 0.46$, indicating a statistically significant degree of covariance ($p = 0.01$, $n = 30$); when there is more descent over Kenya, the equatorial westerlies tend to be stronger, indicating a more pronounced overturning circulation. A dynamical link is hereby demonstrated between Kenyan rainfall and both the local descent and remote ascent at 400 hPa which comprise the vertical components of the Indian Ocean Walker circulation.

The differences between months demonstrate the limitations of considering each rainy season as homogeneous (Nicholson, 2017). Figures 2 and 4 show the variations in ascent and descent at the 400 hPa level, which is the core of both the ascending and descending limbs of the circulation over the Indian Ocean. The climatological descent over Kenya varies in strength between the months, and there is ascent over the Lake Victoria basin in all months (though this is most extensive in April). A more Hadley-like mode is evident in March, but other months show a clear zonal structure between the core ascending regions. There are also differences between the location of the ascending limb over the African continent in October–November versus December; this is located further to the south during December and extends across the Mozambique Channel to Madagascar (Figure 2). Descent at 400 hPa is a consistent feature of the omega climatology over Kenya during both the long and short rains, although there is a greater degree of overturning shown by the streamlines in October–November compared to December. These differences in structure explain why December is

not considered part of the short rains by some authors (Nicholson, 2017), despite being a comparatively wet month. The discontinuity over Kenya of the band of ascending (and thus convergent) air at the equator demonstrates that the widely-held assumption of East African rainfall being primarily controlled by the seasonal migration of the zonal inter-tropical convergence zone (ITCZ) (e.g., Camberlin *et al.*, 2009) may no longer be sufficient given more up-to-date understandings of the tropical rainbelt, which is not exactly co-located with the zone of maximum low-level convergence (Nicholson, 2018).

4 | CMIP5 MODELS

4.1 | Zonal overturning circulations

In our analysis of the coupled models listed in Table 1, we address three questions: are there quantifiable links between the biases in models' representations of Kenyan rainfall and omega over Kenya; what might the similarities be in terms of the convective structure between models that are particularly wet or dry over the country; and do the models behave differently when SST biases are controlled using AMIP runs?

We first examine the extent to which the models can reproduce the observed zonal structure of the Walker circulation with respect to vertical motion. Figure 6 shows the climatological omega across the equatorial Indian Ocean for March and November for the CMIP5 models in Table 1, along with the MERRA-2 reanalysis. The zonal structure revealed in Figure 6 is interesting because of the similarity between March and November, given

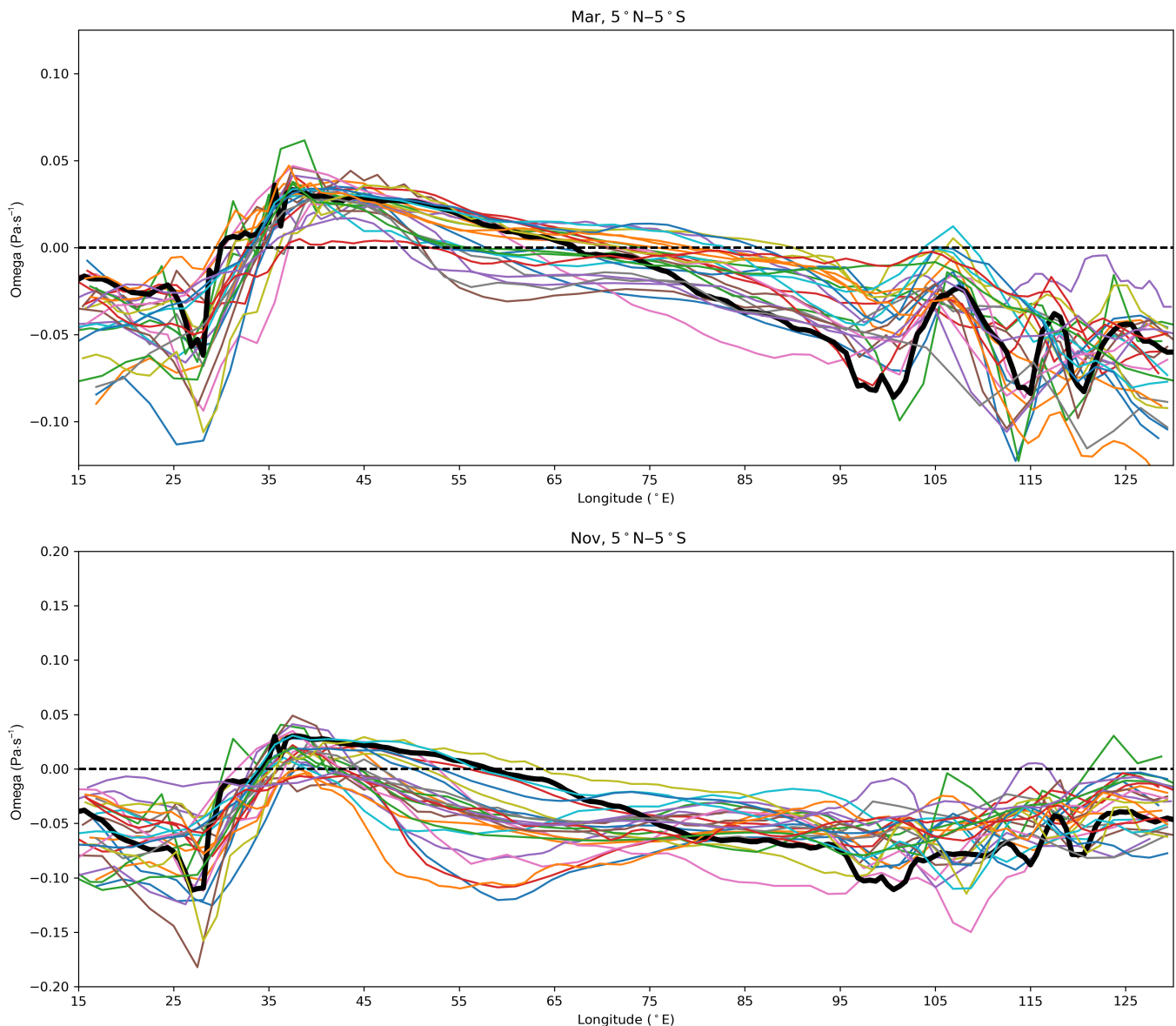


FIGURE 6 400 hPa omega averaged between 5°N–5°S, extending from 15°E–130°E, for March (top) and November (bottom). Each coloured line is a CMIP5 model from Table 1 averaged over 1975–2005 in historical coupled mode. The thick black line is the MERRA-2 reanalysis averaged over 1980–2008. Note different scales

that the canonical overturning circulation is deemed to be active primarily in OND (e.g., Hastenrath *et al.*, 2002). Although the pattern is stronger in November, both months feature ascent over the Maritime Continent and the Congo Basin, and descent over East Africa. While there is substantial inter-model variation as suggested by previous studies on CMIP5 representation of East African climate, the models are in general agreement with the reanalysis pattern.

We examine the climatological zonal overturning circulations in the coupled historical runs of the CMIP5 models listed in Table 1 (Figure 7). We plot the climatological omega and streamlines ($u, w \times 10^4$) for the domain 15°E–130°E, 5°N–5°S during each month in the rainy

seasons, along with biases relative to MERRA-2 (Figure 8). Both figures are arranged based on the climatological rainfall over Kenya, with the driest models at the top left and the wettest models at the top right. For March, the reanalysis data show a clear pattern of ascent over the Maritime Continent and descent over the Western Indian Ocean, with descent in the mid-to-upper troposphere overlying ascent over Kenya (Figure 4). This circulation is represented with varying degrees of accuracy in the CMIP5 ensemble. Figure 7 indicates that drier models tend to overstate both the longitudinal extent and the strength of the descending limb over East Africa. This is consistent with convective inhibition over East Africa and consequently a drier Kenya. For instance, the four

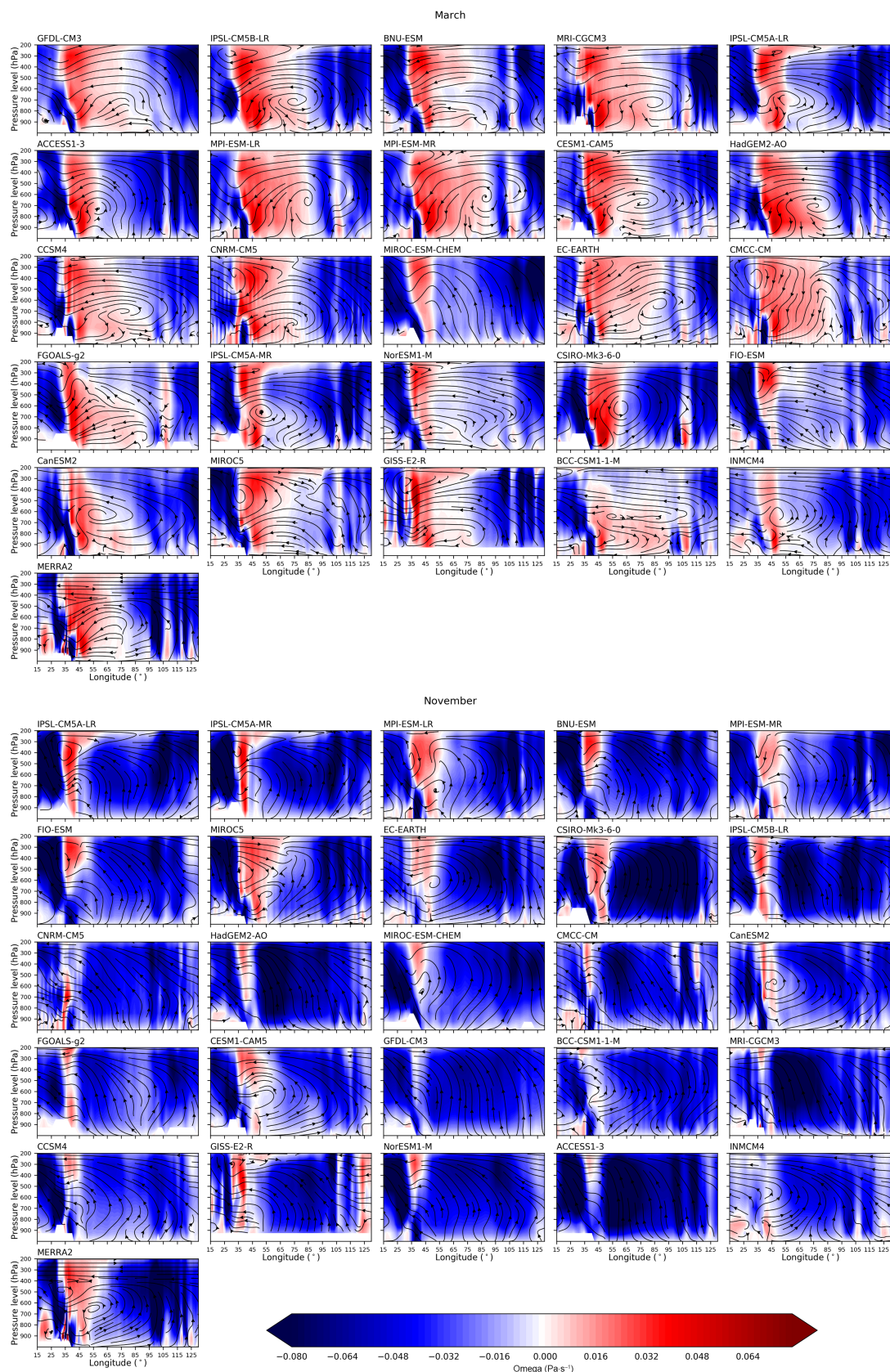


FIGURE 7 As Figure 4, but for March (top) and November (bottom) in the CMIP5 ensemble (Table 1). Models are arranged in rows from driest over Kenya in the given month at the top left, to wettest at the bottom right. MERRA-2 data is included at the bottom left for reference

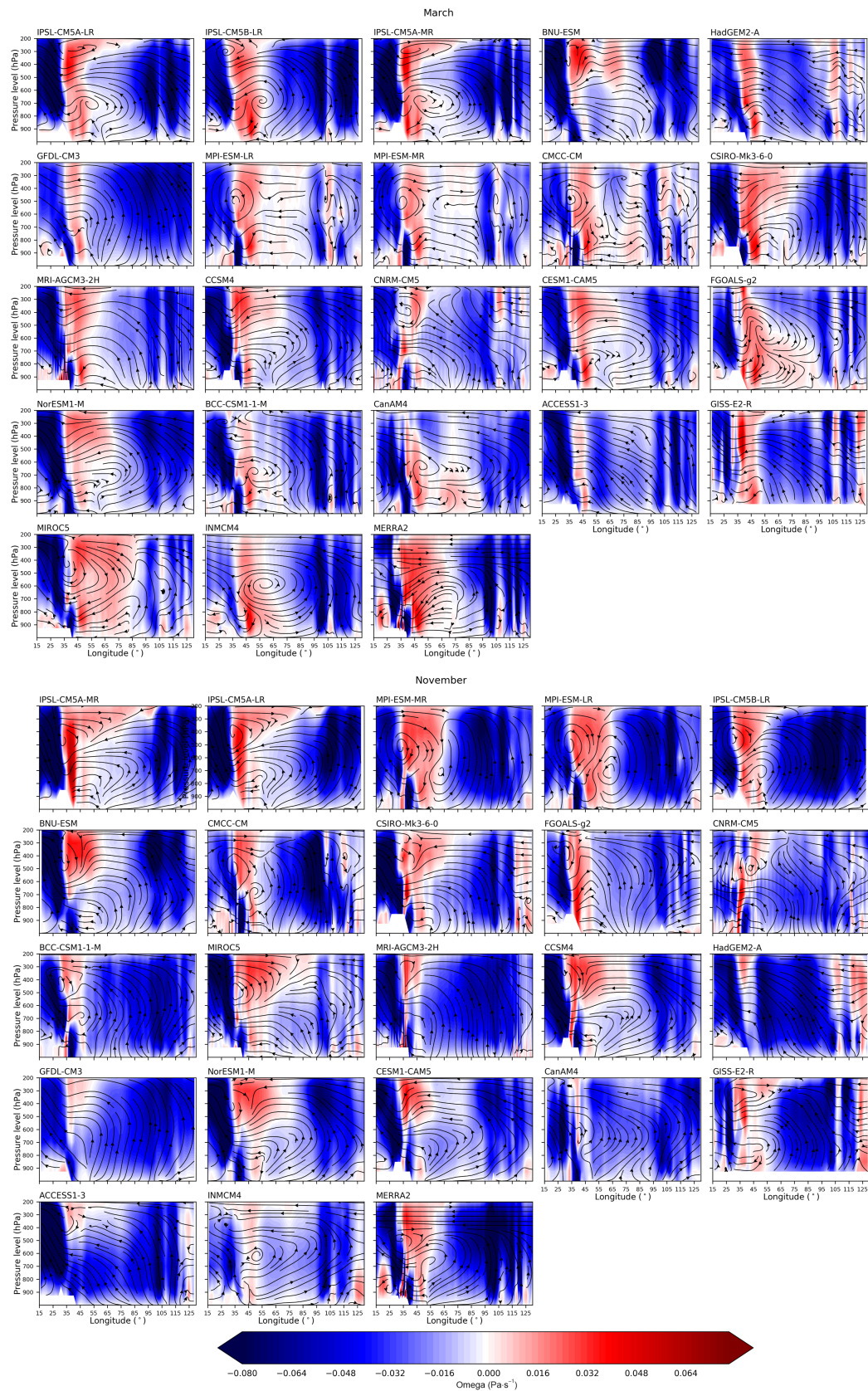


FIGURE 8 As Figure 7, but for the AMIP models in Table 1

driest models extend their descending limbs up to 20° further east than MERRA-2, and are between 4 and 6 times drier than CHIRPSv2.0 over Kenya during this month. On the other hand, the wetter models in the ensemble tend to have much larger regions of ascent extending across the Indian Ocean, weaker descent over East Africa, and in the notable case of BCC-CSM1-1-M, ascent overlying descent across the equatorial IO in a pattern scarcely reminiscent of the canonical zonal overturning circulation. A representative wet model, INMCM4 is 54.9% wetter than CHIRPSv2.0 for this month, has a descending limb which is over 3 times weaker than MERRA-2, and while the strength of its ascending limb is similar to MERRA-2, the model extends the ascent westward by around 25° of longitude. For the AMIP models (Figure 8), some improvements relative to the coupled models are noticeable. In March, the descending limb is more longitudinally constrained across the ensemble, with troposphere-wide descent overlying East Africa and the western Indian Ocean to around 55°E, a comparable extent to MERRA-2. Some models, such as ACCESS1-3, display less realistic motion over the Indian Ocean in AMIP mode than CMIP. Of the four driest (wettest) models in AMIP, 2 (3) were also among the four driest (wettest) models in CMIP.

Simplification of model topography may also be influencing the surface patterns of omega over East Africa, with the localized overturning circulations over land largely absent, and the characteristic vertical structure of surface ascent up to 800 hPa capped by upper-level descent extending throughout the troposphere missing from a number of models. The streamlines indicate that an overturning circulation over the equatorial Indian Ocean is present in a majority of models, but its location is variable. The streamlines at the surface are also indicative of zonal wind biases in a number of models – this has been identified as a key source of model precipitation error in the short rains season by Hiron and Turner (2018), whereby the observed surface westerlies become easterly in some coupled models, leading to erroneous patterns of moisture flux. In terms of the broader

zonal structure of ascent across the Walker circulation in the Western Hemisphere (averaged at the equator from 0° to 200°E), the CMIP5 ensemble mean shows more descending air than reanalysis during the dry-biased long rains months (Table 3), and there is also a significant correlation obtained between the proportion of Western Hemisphere ascending tropospheric air in each model and that model's rainfall over Kenya for November ($R = .409$, $n = 25$, $\alpha = .05$). This implies that models have Walker circulation biases extending beyond the Indian Ocean Basin.

For November, the impact of the Walker circulation is clear (Figure 7). The CMIP5 models generally have wet biases in this month, meaning that the driest models are closest to observed rainfall amounts. These models are close to the reanalysis in terms of their Walker circulation representation, with a broad band of ascent extending throughout the troposphere east of 55°E balanced by descent over Kenya. Even in these models, the core of this descent is narrower by around 10° of longitude and in the driest models extends down to the surface over Kenya. This may lead to increased dry biases over land, and again highlights the impact of model topography on precipitation modelling in this region. The wettest models, by contrast, either feature a greatly reduced zonal overturning circulation, or exhibit a band of ascent extending across the equatorial Indian Ocean and into East Africa in which the Walker circulation is mostly absent. In ACCESS1-3, the region of descent over Kenya found in reanalysis is absent and ascent is found instead; the model's average rainfall for Kenya in November is $5.39 \text{ mm} \cdot \text{day}^{-1}$ compared to $3.06 \text{ mm} \cdot \text{day}^{-1}$ in CHIRPSv2.0. Interestingly, the 3 IPSL models all extend the descending limb to the surface over East Africa – the two configurations of IPSL-CM5A are both substantially drier than observations in November ($1.47 \text{ mm} \cdot \text{day}^{-1}$ for IPSL-CM5A-LR and $1.70 \text{ mm} \cdot \text{day}^{-1}$ for IPSL-CM5A-MR) and across OND.

In the AMIP models, some differences in the structure of the overturning circulation are observed for November (Figure 8). There is an increase in the

TABLE 3 Proportion of ascending versus descending air in the region 0°–200°E, 5°N–5°S, between the surface and 200 hPa

	MERRA2		CMIP5 ensemble ($n = 25$)	
	% ascent	% descent	% ascent	% descent
March	84.74	15.26	73.67	26.33
April	85.91	14.09	76.14	23.86
May	81.32	18.68	77.29	22.71
October	80.20	19.80	77.34	22.66
November	79.26	20.74	80.05	19.95
December	85.70	14.30	79.74	20.26

longitudinal extent of the descending limb of the Walker circulation and a corresponding decrease in the extent of the ascending limb, bringing the models closer to the circulation seen in MERRA-2. Notably, the equatorial westerlies in some models (such as the three IPSL models) are better represented with respect to MERRA-2 than they are in the coupled runs. However, rainfall biases remain, in some cases of opposite signs compared to the coupled versions. For example, CSIRO-MK3-6-0 running in coupled mode has a descending limb which extends around 20° of longitude less than in MERRA-2, and a positive precipitation bias relative to CHIRPS ($+0.29 \text{ mm}\cdot\text{day}^{-1}$). In AMIP mode it exhibits an omega structure which is much closer to MERRA-2, but a negative precipitation bias ($-0.62 \text{ mm}\cdot\text{day}^{-1}$). Of the four driest (wettest) models in AMIP, 3 (3) were also among the four driest (wettest) models in CMIP.

We next considered the structure of CMIP5 vertical motion over the Congo Basin (10°E – 30°E , 5°N – 5°S). This is a key zone of convection driving the Walker circulation and an important moisture source for East Africa. Figure 9 shows a characteristic zone of descending air overlying the Congo Basin below 700 hPa, which is present in all East African rainy season months in reanalysis. This is either underestimated or does not appear in the models. There is also disagreement on the direction of the zonal winds among the models, with some showing surface easterlies and others westerlies. Given that the moisture flux into East Africa from the Congo basin is projected to be of increasing importance in future (Giannini *et al.*, 2018), the realism of these low-level winds warrants further study (though beyond the scope of this article). Related to this is the question of whether or not the low-level subsidence observed in MERRA-2 is realistic. Neupane (2016) did not find this feature in previous generations of reanalysis, but Kuete *et al.* (2019) link vertical velocity at this location to variability in the southern branch of the African Easterly Jet.

The CMIP5 biases in the vertical structure of omega relative to MERRA2 (Figure 10) indicate that models generally underestimate the strength of the zonal overturning circulation in November, with positive biases in the eastern Indian Ocean and negative biases over the west showing that the climatological regions of ascent and descent are both too weak during this month. In March, dry models such as IPSL-CM5B-LR and MRI-CGCM3 are more likely to have descending biases across the Indian Ocean, inhibiting convective potential, whereas wetter models such as BCC-CSM1-1-M and INMCM4 are more likely to have ascending biases. In dry models, the orientation of the streamlines at the 300–400 hPa level in the central Indian Ocean suggests the upper-level easterlies in these models may be too strong,

potentially resulting in a drying mechanism analogous to that described by Williams and Funk (2011).

There is less differentiation between the model biases for November (Figure 10). The models generally have strong omega biases and ascending streamlines over the western and central Indian Ocean throughout the troposphere, indicative of excessive ascent and a weak or absent overturning circulation. The ascent over the Maritime Continent is generally too weak, suggesting that the mechanisms which cause excessive ascent over the Equatorial Indian Ocean are associated with reduced ascent in this region.

The correlations between model rainfall and 400 hPa omega (Figure 11) do, however, suggest that some models are able to capture the spatial structure of the link between the Walker circulation and rainfall (though these should be treated with caution given the biases in both fields). In both March and November, the negative correlation between omega over Kenya and rainfall is observed in all models apart from FGOALS-g2. However, in March models tend to include a narrower than observed band of negative omega/rainfall correlation centred on the equator, which implies a more Hadley-like circulation is acting as a control on rainfall. The existence of this negative correlation extending as far east as the Maritime continent in some of the wetter models (e.g., CanESM2 and MIROC5) supports this implication. For November, the models are less successful at simulating the large region of positive correlation associated with ascent over the Maritime Continent – this is generally less meridionally extensive than in the observations/reanalysis, and is not statistically significant in a number of models.

The CMIP minus AMIP differences (Figure 12) indicate that the strength of the overturning circulation in the coupled models differs between coupled and atmosphere-only configurations. For March, all models in the ensemble show greater descent over East Africa and the western Indian Ocean in CMIP than AMIP, and varying amounts of increased ascent over the Maritime Continent. This indicates a stronger overturning in coupled models than in atmosphere-only models. The reverse is the case for November, where the models exhibit increased ascent across the western Indian Ocean in CMIP relative to AMIP.

Figures 13, 14, and 15 summarize the biases of the CMIP5 models for each rainy season month in precipitation over Kenya (vs. CHIRPS v2.0), 400 hPa omega over Kenya (vs. MERRA-2), and 850 hPa zonal wind over the equatorial Indian Ocean (vs. MERRA-2), respectively. Figure 13 demonstrates the well-known precipitation biases of CMIP5 models over East Africa (e.g., Tierney *et al.*, 2015), namely that MAM rainfall is generally

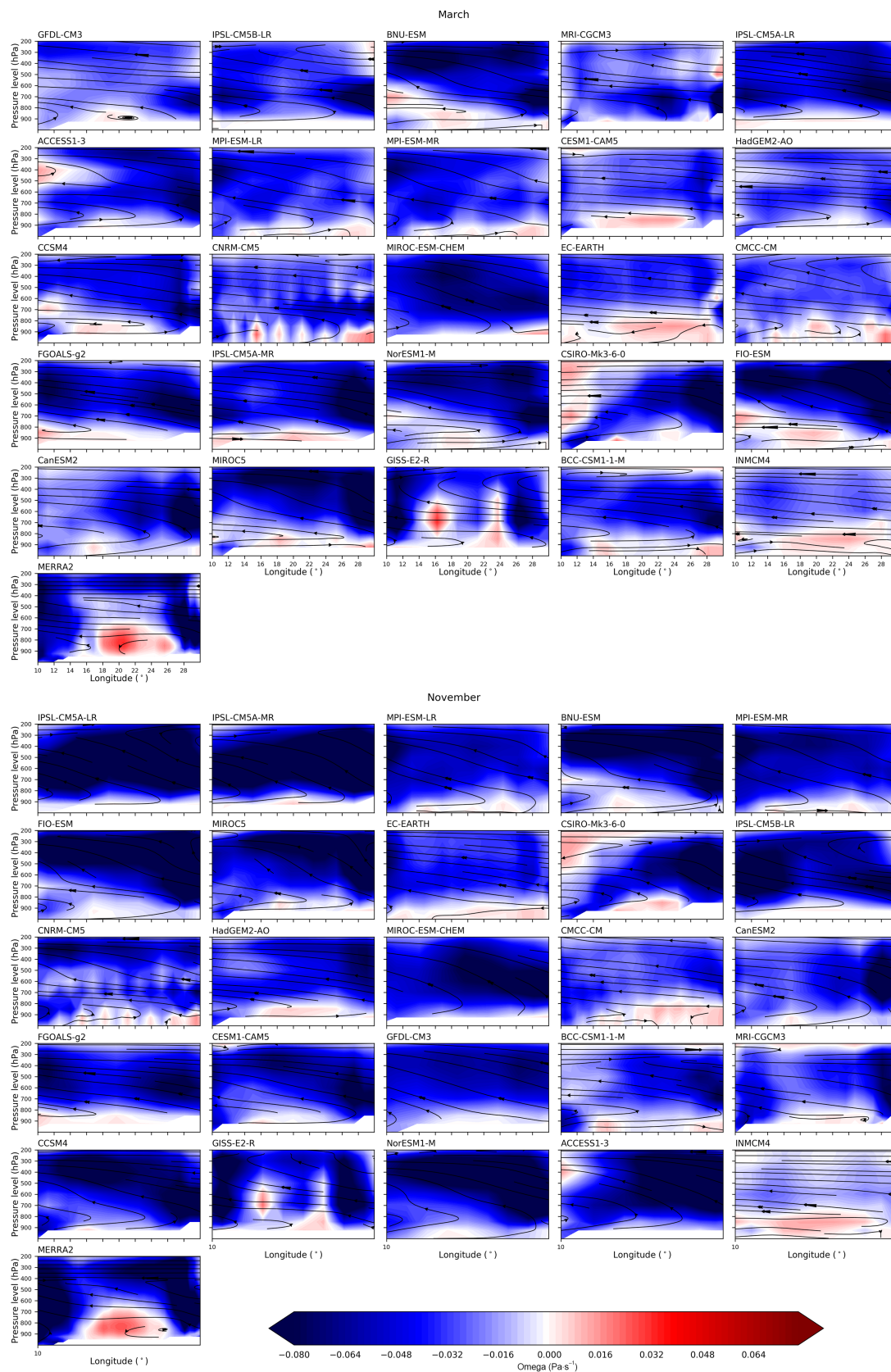


FIGURE 9 As Figure 4, but for the Congo Basin (10° – 30° E, 5° N– 5° S) in March (top) and November (bottom)

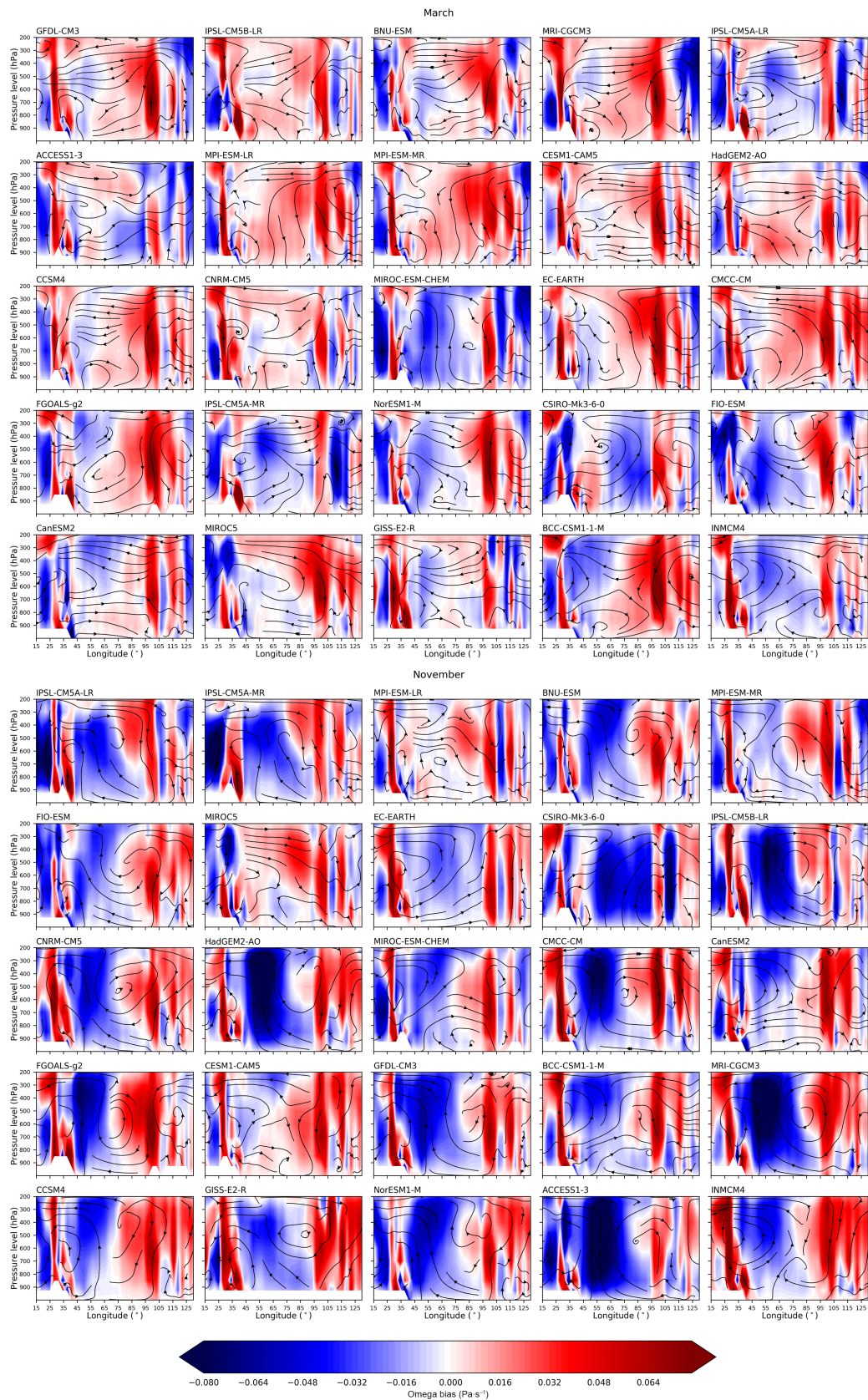


FIGURE 10 As Figure 4, but for model biases relative to MERRA-2 data

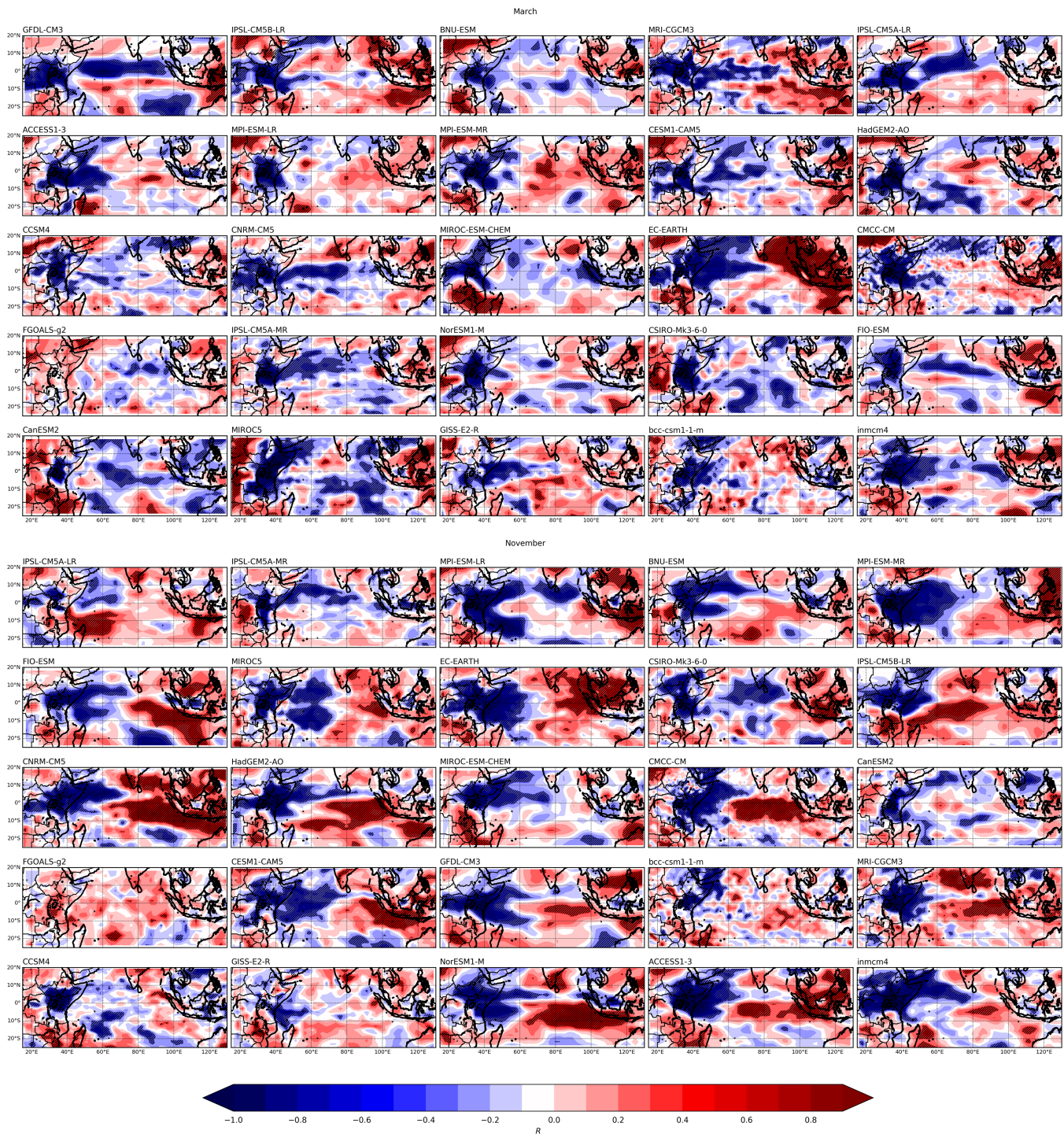


FIGURE 11 Pearson product moment correlation coefficients between CMIP5 model rainfall averaged over Kenya and model 400 hPa omega for March (upper) and November (lower), 1975–2005. Hatching indicates significance at $p < 0.1$. Models are arranged in rows from driest over Kenya in the given month at the top left, to wettest at the bottom right

underestimated while OND rainfall is generally overestimated. Figure 14 supports our contention that these precipitation biases can be understood on climatological timescales as a function of the models' representations of vertical motion associated with the Indian Ocean Walker circulation. In MAM, a majority of models are biased

towards stronger descent over Kenya (positive omega bias), whereas in OND they are biased towards weaker descent or ascent (negative omega bias). Finally, Figure 15 suggests a potential link between the Indian Ocean Walker circulation and MAM rainfall biases as well as OND. As well as extending the findings of Hirons and

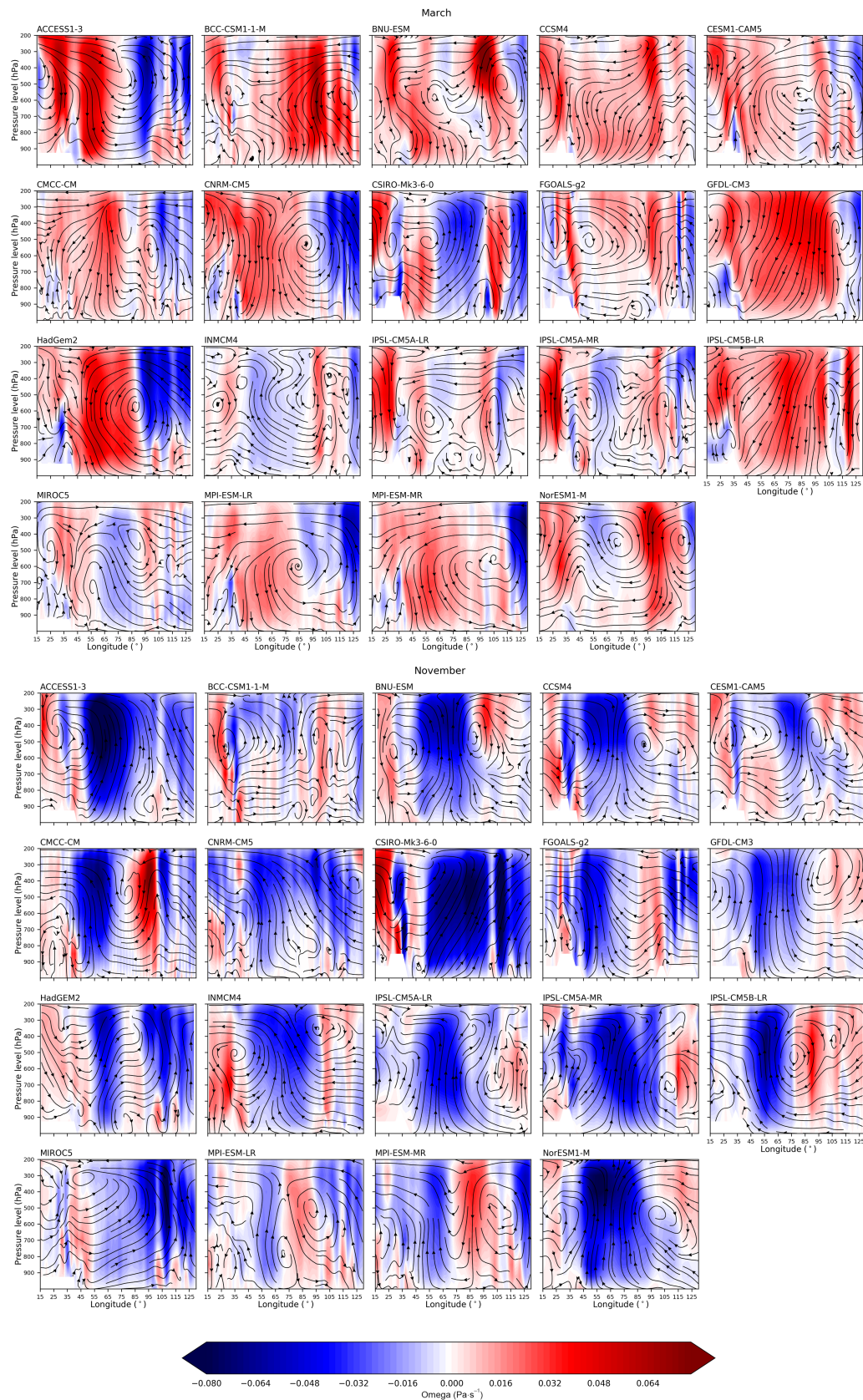
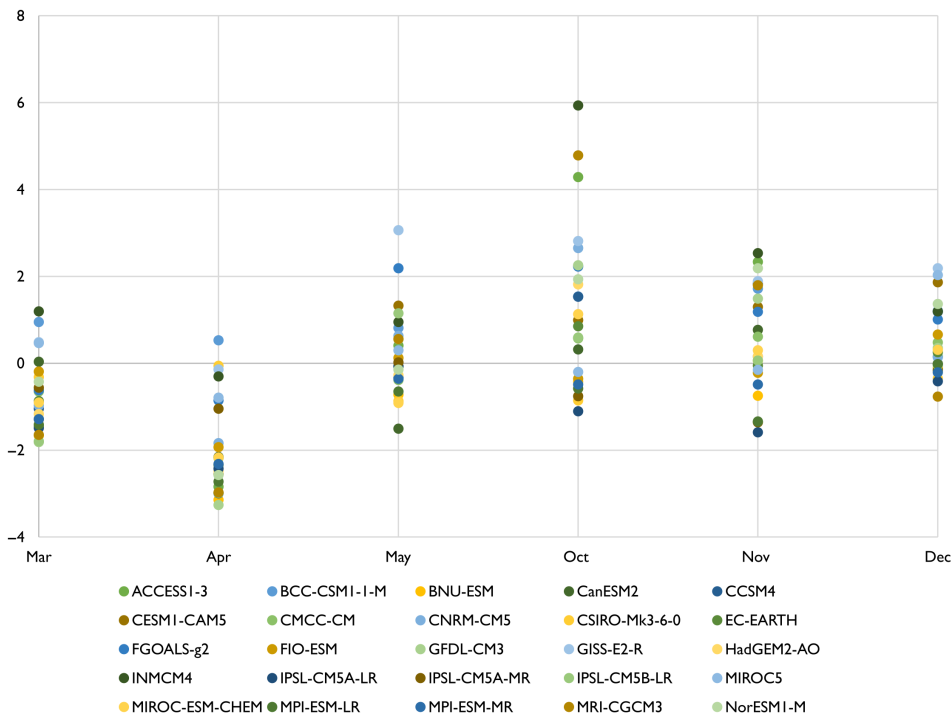
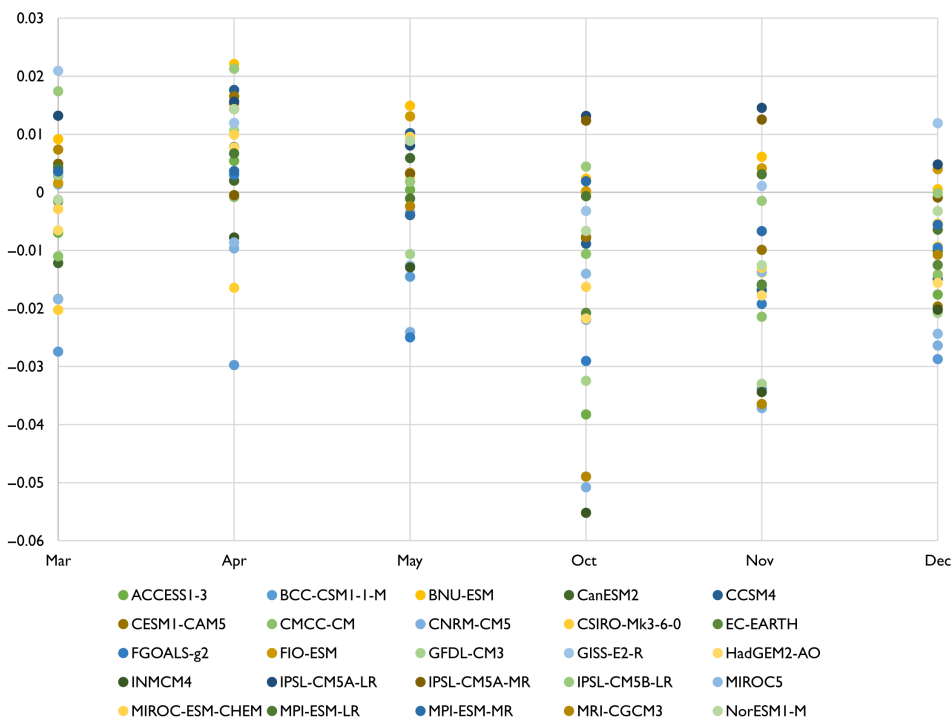


FIGURE 12 Differences between CMIP and AMIP models (CMIP minus AMIP) for March (top) and November (bottom), 1975–2008

Kenya precipitation biases vs. CHIRPSv2.0

**FIGURE 13** CMIP5 model precipitation biases over Kenya for each rainy season month relative to CHIRPSv2.0, 1975–2005

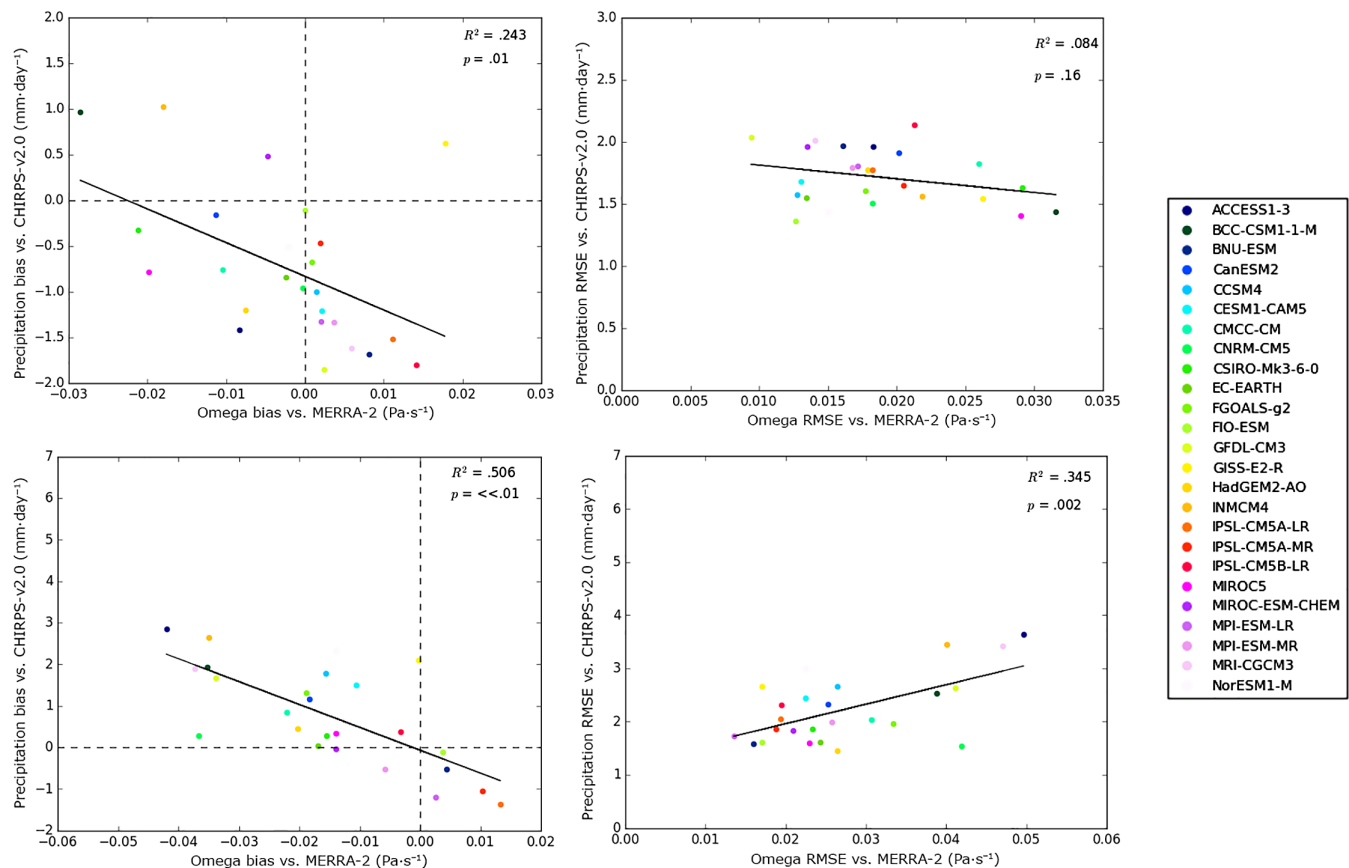
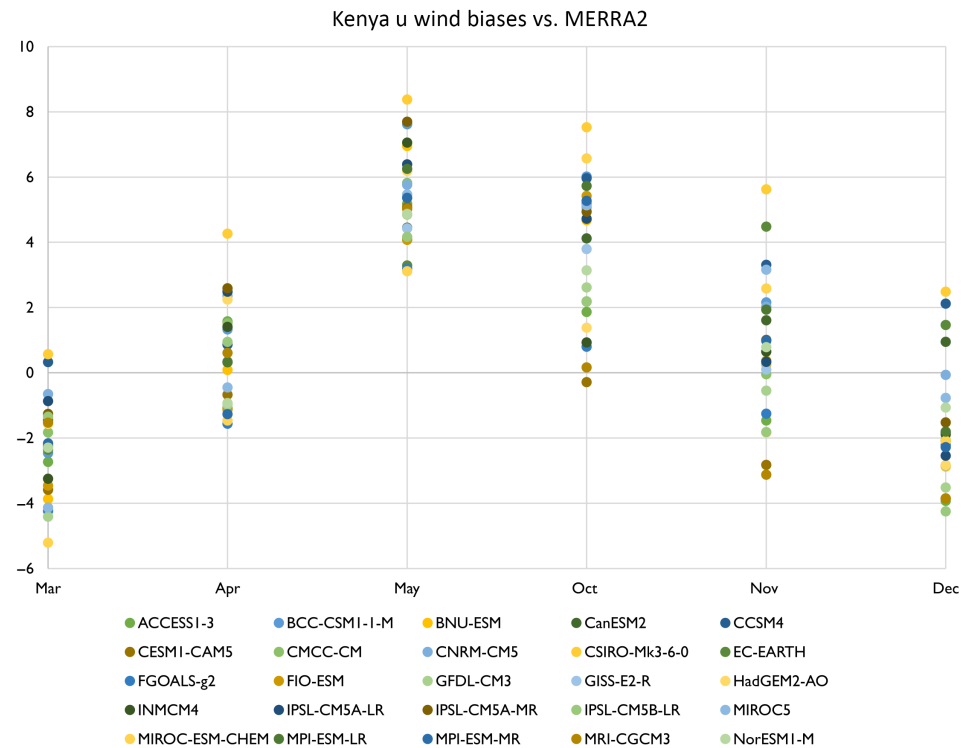
Kenya 400 hPa omega biases vs. MERRA-2

**FIGURE 14** CMIP5 model 400 hPa omega biases over Kenya for each rainy season month relative to MERRA-2 reanalysis, 1980–2005

Turner (2018) that CMIP5 model zonal winds associated with this circulation have easterly biases in OND resulting in anomalously high moisture flux into East Africa, this plot suggests that the reverse is the case in MAM where models tend towards anomalously strong

westerlies. The vertical motion and zonal wind biases have a common direction with respect to East African rainfall, implying that they are part of the same overturning cell. We suggest that further analysis of these wind biases may help resolve the ambiguity in the

FIGURE 15 CMIP5 model 850 hPa zonal wind biases over the equatorial Indian Ocean (50°E–100°E, 5°N–5°S) for each rainy season month relative to MERRA-2 reanalysis, 1980–2005



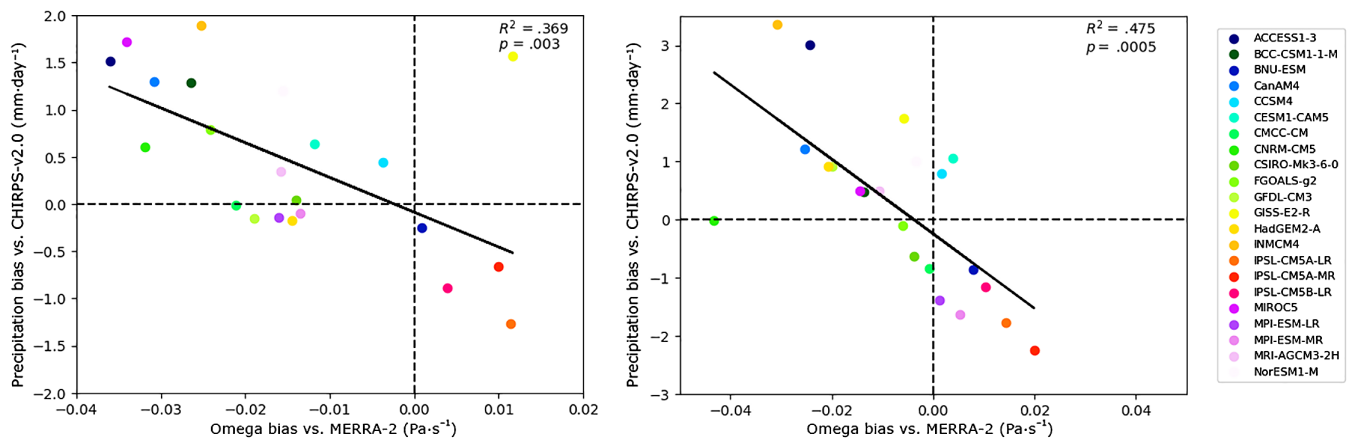


FIGURE 17 Relationship between model biases in rainfall and 400 hPa omega over Kenya for March (left) and November (right) in AMIP models. Note different scales

literature on the role of the Indian Ocean Walker circulation during the long rains.

We next plot the model biases in precipitation over Kenya (relative to CHIRPS v2.0) against the model biases in omega (relative to MERRA-2) for each month over the period 1981–2005. We also plot RMSE (Equation 1) in precipitation against RMSE in omega for the same period.

$$RMSE = \sqrt{\frac{\sum_{t=1}^T (x_{1,t} - x_{2,t})^2}{T}}$$

Figure 16 indicates that there is a relationship between model biases in the descending limb of the Walker circulation over Kenya and rainfall over Kenya. Models with stronger descent (positive omega bias) over Kenya are also generally drier (negative rainfall bias), dependent on the rainy season month. During the long rains, the relationship holds for March ($R^2 = .243$, $p = .01$), April ($R^2 = .201$, $p = .02$), and May ($R^2 = .341$, $p = .002$). During the short rains, there is a strong relationship in October ($R^2 = .728$, $p = 6 \times 10^{-8}$) and November ($R^2 = .506$, $p = 7 \times 10^{-5}$) but not December ($R^2 = .025$, $p = .45$). This relationship is also present in the AMIP models (Figure 17) in both March ($R^2 = .369$, $p = .003$) and November ($R^2 = .475$, $p = .0005$). In AMIP, models in March tend towards wet biases, in opposition to CMIP. In November, there is an equal spread of dry and wet biased models in AMIP, whereas CMIP models tend towards wet biases.

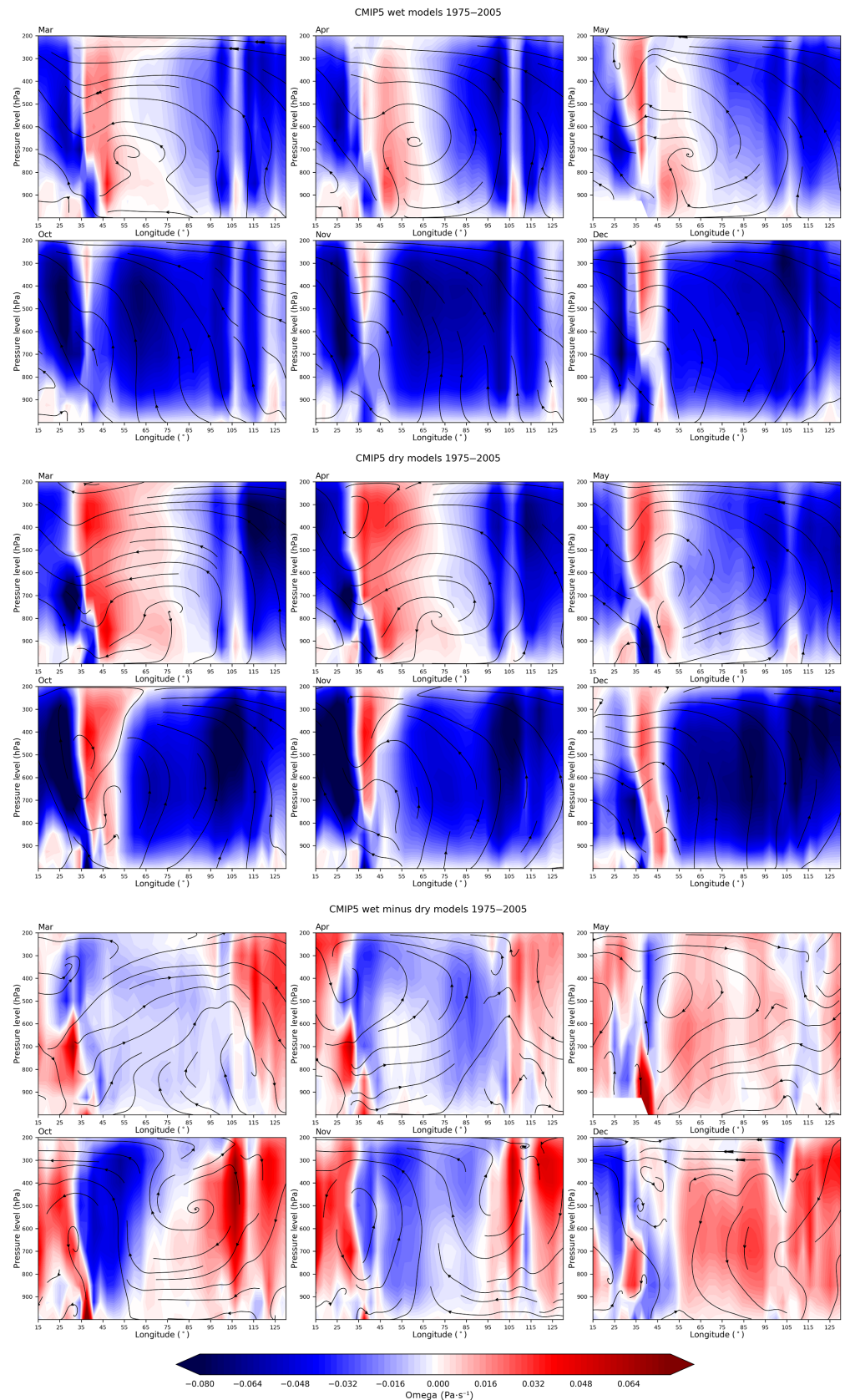
The RMSE plots in Figure 16 give a more general indication of the links between model biases by removing the directionality of the relationship shown in the bias plots, in order to assess whether low error in omega is associated with low error in rainfall relative to the reference datasets. In this case, the relationship is not

significant in any of the long rains months, but is both significant and positive in the short rains. This indicates that models with greater biases in Kenya omega during OND also have greater biases in Kenya rainfall. In the long rains months, several models have low RMSE in precipitation but also high RMSE in omega. This suggests that although these models are successful at reproducing observed rainfall statistics, their dynamics are potentially less realistic. These models include: BCC-CSM1-1-M, GISS-E2-R, INMCM4, and MIROC5 (March); BCC-CSM1-1-M, CSIRO-Mk3-6-0, FGOALS-g2, MIROC5, and MPI-ESM-LR (April); and CNRM-CM5 and NorESM1-M (May). In the short rains months, the link between RMSE in precipitation and in omega is stronger. With the exception of CNRM-CM5 during November/December and GFDL-CM3 in December, there are no models exhibiting low RMSE in precipitation with high RMSE in omega; rather, models tend to have correspondingly high or low error values in both variables. It is noteworthy that several of the models which have ‘good’ rainfall but ‘bad’ omega during the long rains are ‘bad’ in both variables during short rains months (including INMCM4 and FGOALS-g2). These models generally exhibit strong wet biases in OND. They are also among the wettest models in the ensemble for MAM, but since the ensemble as a whole is drier than observations during this season, these models return a low RMSE score. This suggests a link between the underlying model processes causing wet biases in both rainy seasons.

4.2 | Wet versus dry models

The composites of the four driest CMIP5 models in monthly averages for each rainy season month (Figure 18 middle panel) further suggest a role for the

FIGURE 18 As Figure 4, but for composite averages of the wettest four CMIP5 models in each month (top); the driest four models (middle); and the wet composites minus the dry composites (bottom)



Walker circulation. The models are generally too dry in the long rains and too wet in the short rains, with 75% of models being too dry during MAM and 65% of

models being too wet in OND. The composites show much more extensive descent and more pronounced overturning circulations over the western Indian

Ocean and East Africa in March and April relative to OND. In the short rains dry model composite, the overturning circulations are weaker and shallower – though these dry models are closer to observed values

of rainfall, the structures by which the rainfall is produced can thus be called into question.

For the wet composites, a similar picture emerges. The wet models in MAM show markedly less descent

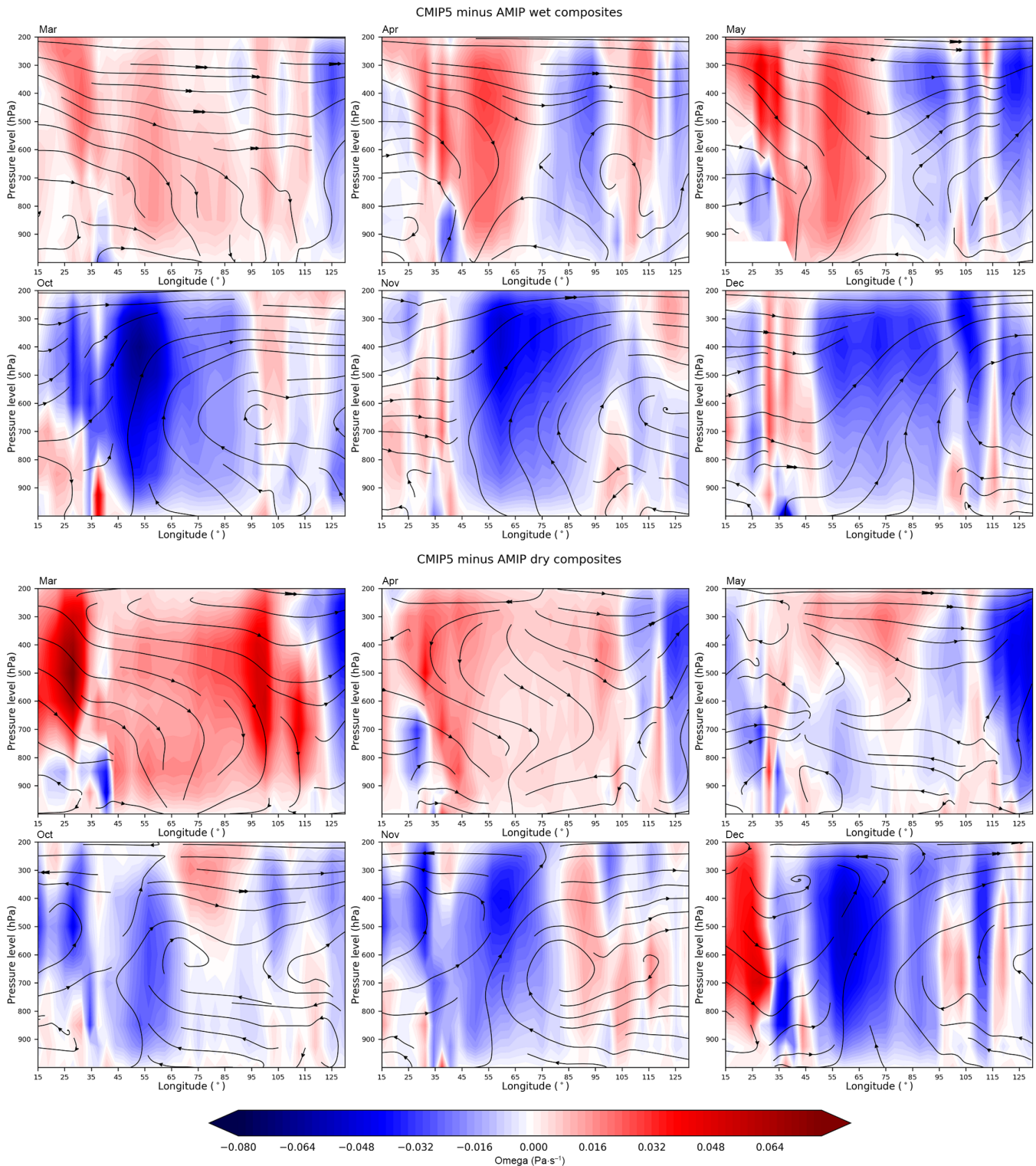


FIGURE 19 Differences between the wettest CMIP and AMIP models for the rainy season months (top) and between the driest CMIP and AMIP models (bottom)

over East Africa and less ascent over the Maritime Continent, with an additional band of ascent between 40°E–45°E (Figure 18, top panel). During the short rains (especially October and November), there is little evidence of an overturning circulation in the wet composites, with the easterly orientation of the streamlines at the surface indicative of zonal wind biases over the equatorial Indian Ocean. The wet minus dry composites indicate a role for the Walker circulation over the Indian Ocean, with wet models characterized by a weaker descent over East Africa, weaker ascent over the Maritime Continent, and erroneous zonal winds in the lower troposphere (Figure 18, bottom panel). This picture is supported by the differences between composites of the driest and wettest CMIP and AMIP models (Figure 19). In MAM, when CMIP5 exhibits a dry bias, the coupled model dry composites have more descent over the domain than the atmosphere-only dry composites. The reverse is true for the wet composites in OND, when CMIP wet models have increased ascent over the domain compared to AMIP.

5 | SUMMARY AND CONCLUSION

5.1 | Summary of Walker circulation impacts on Kenyan rainfall

CMIP5 models exhibit well-known biases over Kenya, and East Africa more generally. They underestimate the magnitude of rainfall during the long rains (MAM), some by over half, and overestimate rainfall during the short rains (OND), some by over 100%. There is also a general spring wetting trend in CMIP5 projections which has been questioned given the observed multi-decadal drying trend in the region. In this study, we show that the models' representations of the zonal Walker circulation over the equatorial Indian Ocean are unrealistic. Most models simulate the descending limb of the Walker cell over the western Indian Ocean and East Africa during the long rains months in a too strong and too extensive manner compared to the MERRA-2 reanalysis (Figure 10), inhibiting convective potential over East Africa and potentially leading to positive low-to-mid tropospheric pressure anomalies which may inhibit the advection of warm moist air from the eastern Indian Ocean. This behaviour is apparent in the dry/wet composites (Figure 18), in which the dry models for MAM have stronger and more extensive descent over East Africa, and a more clearly defined zonal overturning circulation, than the wet models in the same months. This picture is consistent with a dry bias over Kenya during the long rains season, although the circulation is less well

defined during this season (Liebmann *et al.*, 2017). However, Figure 6 indicates that the zonal structure of vertical motion over the equatorial Indian Ocean is similar in both rainy seasons, with ascent over the Maritime Continent and the Congo Basin balanced by descent over East Africa. This descent acts to dampen deep convection over East Africa, and may contribute towards the relative aridity of Kenya compared to other regions on the equator. We encourage further research to develop a more precise definition of the seasonal cycle of the Indian Ocean Walker circulation.

During the short rains season, 19/25 models either underestimate the overturning cell or miss it out entirely (Figure 7). In November, four models feature a Hadley Cell-like band of almost uniform convection extending throughout the troposphere, rather than the characteristic pattern of ascent in the east and descent in the west seen in reanalysis. This broad convection over the equatorial Indian Ocean, when combined with warming SSTs in the Indian Ocean, could increase moisture availability for East African rainfall – when combined with the mean-state zonal wind biases found in coupled models by Hirons and Turner (2018), in which models produce surface easterlies rather than the observed westerlies, this would increase moisture flux into East Africa and result in a substantially wetter short rains season. Models are known to have biases in the Indian Ocean Dipole during OND (Cai and Cowan, 2013), and this has been shown to be connected to their representations of the Walker circulation (Hirons and Turner, 2018). More work is needed to further disentangle the relationship between omega, wind, and SST biases, and their respective controls on East African rainfall in CMIP5 models. Given that CMIP5 rainfall biases over the Congo Basin are associated with differences in moisture flux (Washington *et al.*, 2013), the representations of omega and zonal wind over the region shown in Figure 6 warrant further investigation. Models with divergent moisture flux over the Congo Basin are dry in that region (Washington *et al.*, 2013), but may also transport more of that moisture to East Africa. For example, the model identified by Washington *et al.* (2013) as the driest over the Congo in SON (CNRM-CM5) is the fifth-wettest over East Africa in October. The location of the boundary between Congo ascending air and East African descending air may be one of the key factors determining whether a climate model, and indeed an observed rainy season, is particularly wet or dry over East Africa. On a global scale, Table 3 suggests that further investigation into CMIP5 equatorial vertical motion may reveal biases towards descending air in MAM, with implications for rainfall elsewhere in the Tropics.

The comparison between AMIP and CMIP models suggests that the Walker circulation biases in coupled

models are at least partially attributable to the SST biases known to be an issue in CMIP5. When SST is controlled, models have less strong descent over the Western Indian Ocean during the long rains, and less strong ascent over the same region during the short rains. An improvement in the representation of equatorial westerlies over the Indian Ocean during November is a notable feature of the AMIP models (Figure 8). This is consistent with a correction to the positive IOD-like SST bias exhibited by CMIP5 models, though it should also be noted that AMIP models cannot represent the nature of the IOD and its associated westerlies as a coupled ocean–atmosphere system.

5.2 | Implications for future model projections

Models have biases in the mean state of the Walker circulation over the Indian Ocean, with consequent impacts on their representation of rainfall over Kenya. While this study focusses on the historical coupled simulations of CMIP5, its findings are relevant to the interpretation of these models' projections of future rainfall in the region under anthropogenic climate change (Yang *et al.*, 2014). It is not sufficient to base assessments of the reliability of models' future rainfall projections on their rainfall output alone (James *et al.*, 2015). Models which have unrealistic dynamics related to a projected variable of interest in historical coupled simulations (for which they can be assessed against observations) cannot be considered reliable sources of climate projections. Conversely, those models which do have accurate dynamics can be considered more reliable in their future projections. This process-based approach to climate model evaluation is useful both for selecting projections from specific models in the absence of a physically plausible signal in the ensemble mean (Creese and Washington, 2016), and for assessing which global climate models are most suitable for use in regional downscaling experiments (McSweeney *et al.*, 2015). While this article does not explicitly address the effect of model resolution, this might also provide some insights into the reasons behind the differences in model circulations; preliminary analysis indicated a weak but significant relationship between model resolution and the strength of ascent over the Maritime Continent in November (not shown), and this could be linked to the broader circulation. Recent experiments using a high-resolution convection-permitting regional model over East Africa have yielded improvements in the representation of rainfall in the area (Finney *et al.*, 2019); driving such a model with more realistic large-scale flow at the boundaries of the regional simulation could lead to additional such improvements. Additionally, the strong

correlations obtained between omega and rainfall in all rainy season months could benefit seasonal forecasting of rainfall in East Africa, which historically has been more difficult for the long rains owing to a lack of reliable teleconnections (MacLeod, 2018; Walker *et al.*, 2019).

The improvements yielded by AMIP in simulating the current Walker circulation structure over the Indian Ocean suggest that coupled models may not yield reliable projections of future climate in the region. It follows that projections made by applying a Δ SST function to observed data (i.e., adding a warming factor to provide forcing rather than simulating the ocean explicitly) may have value in this region – especially when combined with the high-resolution regional models now available such as that of Stratton *et al.* (2018). However, care should be taken in the interpretation of such experiments, since the IOD and ENSO are coupled ocean–atmosphere systems and future changes in their behaviour, which are unlikely to simply be a linear warming of their current states, would affect East African rainfall.

In this article, we have addressed three questions. First, we quantified the relationship between the Indian Ocean Walker circulation and Kenyan rainfall using reanalysis and gridded rainfall. Next, the representation of the zonal Walker circulation over the equatorial Indian Ocean in CMIP5 models was investigated, and found to differ substantially from the MERRA-2 reanalysis. Finally, we examined the models' Walker circulation/rainfall relationships in the context of known CMIP5 rainfall biases. These models have rainfall biases over East Africa which can be accounted for as a result of the Walker circulation biases – in particular, the wet bias during the short rains is associated with a significantly reduced overturning circulation in most models, and the dry bias during the long rains with excessive subsidence over East Africa. The mean state of the Walker circulation in the models is therefore not that which is seen in reanalysis. Consequently, projections of Kenyan rainfall made using these models are derived from forcings applied to an erroneous baseline. This means that their future projections may not be plausible. Future work will consider whether models with distinctly realistic or unrealistic Walker circulations in the historical coupled runs project distinctly different future rainfall signals. Additionally, the influence of model topography on East African rainfall requires further study, particularly with regard to low-level convection, moisture flux (convergence), and the influence of the Turkana low-level jet. More work is needed to further disentangle the relationship between omega, wind, and SST biases, and their respective controls on East African rainfall, as well as the impact of the Walker circulation in observations and models in other parts of the Tropics.

ACKNOWLEDGEMENTS

James A. King is funded by the UK Natural Environment Research Council (NERC) through the Doctoral Training Partnership in Environmental Research (grant NE/L002621/1). This work forms part of his doctoral thesis. The CMIP5 data used in this study were downloaded from the UK Centre for Environmental Data Analysis (CEDA), (<https://catalogue.ceda.ac.uk/uuid/d2d8f982d66cce55bb59fc769ca39264?jump=related-docs-anchor>). CHIRPS rainfall data were downloaded from the Climate Hazards Group at the University of California, Santa Barbara. (ftp://ftp.chg.ucsb.edu/pub/org/chg/products/CHIRPS-2.0/global_monthly/netcdf/). MERRA-2 data were downloaded from the NASA Goddard Earth Sciences Data and Information Services Centre (<https://disc.gsfc.nasa.gov/datasets?keywords=%22MERRA-2%22&page=1&source=Models%2FAnalyses%20MERRA-2>). The authors thank Ellen Dyer, Dave MacLeod, David Crowhurst, and Callum Munday for their valuable input. The comments of two anonymous reviewers helped improve the manuscript.

ORCID

James A. King  <https://orcid.org/0000-0001-8825-0183>

REFERENCES

- Behera, S.K., Luo, J.-J., Masson, S., Delecluse, P., Gualdi, S., Navarra, A. and Yamagata, T. (2005) Paramount impact of the Indian Ocean Dipole on the East African short rains: a CGCM study. *Journal of Climate*, 18, 4514–4530.
- Berhane, F. and Zaitchik, B. (2014) Modulation of daily precipitation over East Africa by the Madden-Julian oscillation. *Journal of Climate*, 27, 6016–6034.
- Black, E. (2005) The relationship between Indian Ocean Sea-surface temperature and East African rainfall. *Philosophical Transactions of the Royal Society A*, 363, 43–47.
- Black, E., Slingo, J. and Sperber, K.R. (2003) An observational study of the relationship between excessively strong short rains in coastal East Africa and Indian Ocean SST. *Monthly Weather Review*, 131, 74–94.
- Borgomeo, E., Vadheim, B., Woldeyes, F.B., Alamirew, T., Tamru, S., Charles, K.J., Kebede, S. and Walker, O. (2018) The distributional and multi-sectoral impacts of rainfall shocks: evidence from computable general equilibrium modelling for the Awash Basin, Ethiopia. *Ecological Economics*, 146, 621–632.
- Cai, W. and Cowan, T. (2013) Why is the amplitude of the Indian Ocean Dipole overly large in CMIP3 and CMIP5 models? *Geophysical Research Letters*, 40, 1200–1205.
- Camberlin, P., Moron, V., Okoola, R., Philippon, N. and Gitau, W. (2009) Components of rainy seasons' variability in equatorial East Africa: onset, cessation, rainfall frequency and intensity. *Theoretical and Applied Climatology*, 98, 237–249.
- Chadwick, R., Boutle, I. and Martin, G. (2013) Spatial patterns of precipitation change in CMIP5: why the rich do not get richer in the Tropics. *Journal of Climate*, 26, 3803–3822.
- Collier, P., Conway, G. and Venables, T. (2008) Climate change and Africa. *Oxford Review of Economic Policy*, 24, 337–353.
- Collins, M., Minobe, S., Barreiro, M., Bordoni, S., Kaspi, Y., Kuwano-Yoshida, A., Keenlyside, N., Manzini, E., O'Reilly, C. H., Sutton, R., Xie, S.-P. and Zolina, O. (2018) Challenges and opportunities for improved understanding of regional climate dynamics. *Nature Climate Change*, 8, 101–108.
- Creese, A. and Washington, R. (2016) Using qflux to constrain modeled Congo Basin rainfall in the CMIP5 ensemble. *Journal of Geophysical Research – Atmospheres*, 121, 13415–13442.
- Dawson, A. (2016) Windspharm: a high-level library for global wind field computations using spherical harmonics. *Journal of Open Research Software*, 4, e31. <https://doi.org/10.5334/jors.129>.
- Diro, G.T., Grimes, D.I.F. and Black, E. (2011) Teleconnections between Ethiopian summer rainfall and sea surface temperature: part 1 – observation and modelling. *Climate Dynamics*, 37, 103–119.
- Dunning, C.M., Black, E.C.L. and Allan, R.P. (2016) The onset and cessation of seasonal rainfall over Africa. *Journal of Geophysical Research – Atmospheres*, 121, 11405–11424.
- Endris, H.S., Lennard, C., Hewitson, B., Dosio, A., Nikulin, G. and Artan, G.A. (2018) Future changes in rainfall associated with ENSO, IOD and changes in the mean state over eastern Africa. *Climate Dynamics*, 52, 2029–2053. <https://doi.org/10.1007/s00382-018-4239-7>.
- Finney, D., Marsham, J., Jackson, L., Kendon, E., Rowell, D., Boorman, P., Keane, R. and Senior, C. (2019) Implications of improved representation of convection for the East Africa water budget using a convection-permitting model. *Journal of Climate*, 32, 2109–2129. <https://doi.org/10.1175/JCLI-D-18-0387.1>.
- Funk, C., Dettlinger, M.D., Michaelsen, J.C., Verdin, J.P., Brown, M. E., Barlow, M. and Hoell, A. (2008) Warming of the Indian Ocean threatens eastern and southern African food security but could be mitigated by agricultural development. *Proceedings of the National Academy of Sciences of the United States of America*, 105, 11081–11086.
- Funk, C., Peterson, P., Landsfeld, M., Pedreros, D., Verdin, J., Shukla, S., Husak, G., Rowland, J., Harrison, L., Hoell, A. and Michaelsen, J. (2015) The climate hazards infrared precipitation with stations – a new environmental record for monitoring extremes. *Scientific Data*, 2, 150066. <https://doi.org/10.1038/sdata.2015.66>.
- Gebrechorkos, S.H., Hülsmann, S. and Bernhofer, C. (2018) Evaluation of multiple climate data sources for managing environmental resources in East Africa. *Hydrology and Earth System Sciences*, 22, 4547–4564.
- Gelaro, R., McCarty, W., Suárez, M.J., Todling, R., Molod, A., Takacs, L., Randles, C.A., Darmenov, A., Bosilovich, M.G., Reichle, R., Wargan, K., Coy, L., Cullather, R., Draper, C., Akella, S., Buchard, V., Conaty, A., da Silva, A.M., Gu, W., Kim, G., Koster, R., Lucchesi, R., Merkova, D., Nielsen, J.E., Partyka, G., Pawson, S., Putman, W., Rienecker, M., Schubert, S.D., Sienkiewicz, M. and Zhao, B. (2017) The modern-era retrospective analysis for research and applications, version 2 (MERRA-2). *Journal of Climate*, 30, 5419–5454.
- Giannini, A., Lyon, B., Seager, R. and Vigaud, N. (2018) Dynamical and thermodynamic elements of modelled climate change at the East African margin of convection. *Geophysical Research Letters*, 45, 992–1000.
- Hart, N.C.G., Washington, R. and Stratton, R.A. (2018) Stronger local overturning in convective-permitting regional climate

- model improves simulation of the subtropical annual cycle. *Geophysical Research Letters*, 45, 11334–11342.
- Hartman, A.T. (2018) An analysis of the effects of temperatures and circulations on the strength of the low-level jet in the Turkana Channel in East Africa. *Theoretical and Applied Climatology*, 132, 1003–1017.
- Hastenrath, S., Polzin, D. and Greischar, L. (2002) Annual cycle of equatorial zonal circulations from the ECMWF reanalysis. *Journal of the Meteorological Society of Japan. Ser. II*, 80, 755–766.
- Hession, S.L. and Moore, N. (2011) A spatial regression analysis of the influence of topography on monthly rainfall in East Africa. *International Journal of Climatology*, 31, 1440–1456.
- Hirons, L. and Turner, A. (2018) The impact of Indian Ocean mean-state biases in climate models on the representation of the East African short rains. *Journal of Climate*, 31, 6611–6631.
- Hoell, A., Funk, C. and Barlow, M. (2014) La Niña diversity and Northwest Indian Ocean rim teleconnections. *Climate Dynamics*, 43, 2707–2724.
- Hoell, A., Hoerling, M., Eischeid, J., Quan, X.-W. and Liebmann, B. (2017) Reconciling theories for human and natural attribution of recent East Africa drying. *Journal of Climate*, 30, 1939–1956.
- Hua, W., Zhou, L., Nicholson, S.E., Chen, H. and Qin, M. (2019) Assessing reanalysis data for understanding rainfall climatology and variability over central equatorial Africa. *Climate Dynamics*, 53, 651–669. <https://doi.org/10.1007/s00382-018-04604-0>.
- James, R., Washington, R. and Jones, R. (2015) Process-based assessment of an ensemble of climate projections for West Africa. *Journal of Geophysical Research – Atmospheres*, 120, 1221–1238.
- James, R., Washington, R., Abiodun, B., Kay, G., Mutemi, J., Pokam, W., Hart, N., Artan, G. and Senior, C. (2018) Evaluating climate models with an African lens. *Bulletin of the American Meteorological Society*, 99, 313–336.
- Kaunda, C.S., Kimambo, C.Z. and Nielsen, T.K. (2012) Potential of small-scale hydropower for electricity generation in sub-Saharan Africa. *ISRN Renewable Energy*, 2012. <https://doi.org/10.5402/2012/132606>.
- Kimani, M.W., Hoedjes, J.C.B. and Su, Z. (2017) An assessment of satellite-derived rainfall products relative to ground observations over East Africa. *Remote Sensing*, 9, 430–450. <https://doi.org/10.3390/rs9050430>.
- Kociuba, G. and Power, S.B. (2015) Inability of CMIP5 models to simulate recent strengthening of the Walker circulation: implications for projections. *Journal of Climate*, 28, 20–35.
- Kuete, G., Mba, W.P. and Washington, R. (2019) African easterly jet south: control, maintenance mechanisms and link with southern subtropical waves. *Climate Dynamics*, 54, 1539–1552.
- L'Heureux, M.L., Lee, S. and Lyon, B. (2013) Recent multidecadal strengthening of the Walker circulation across the tropical Pacific. *Nature Climate Change*, 3, 571–576.
- Li, G. and Xie, S.-P. (2014) Tropical biases in CMIP5 multimodel ensemble: the excessive equatorial Pacific cold tongue and double ITCZ problems. *Journal of Climate*, 27, 1765–1780.
- Li, T., Zhang, L. and Murakami, H. (2015) Strengthening of the Walker circulation under global warming in an aqua-planet general circulation model simulation. *Advances in Atmospheric Sciences*, 32, 1473–1480.
- Liebmann, B., Hoerling, M.P., Funk, C., Bladé, I., Dole, R.M., Allured, D., Quan, X., Pegion, P. and Eischeid, J.K. (2014) Understanding recent Eastern Horn of Africa rainfall variability and change. *Journal of Climate*, 27, 8630–8645.
- Liebmann, B., Bladé, I., Funk, C., Allured, D., Quan, X., Hoerling, M., Hoell, A., Peterson, P. and Thiaw, W.M. (2017) Climatology and interannual variability of boreal spring wet season precipitation in the Eastern Horn of Africa and implications for its recent decline. *Journal of Climate*, 30, 3867–3886.
- Lyon, B. (2014) Seasonal drought in the greater horn of Africa and its recent increase during the March–May long rains. *Journal of Climate*, 27, 7953–7975.
- MacLeod, D. (2018) Seasonal predictability of onset and cessation of the East African rains. *Weather and Climate Extremes*, 21, 27–35.
- MacLeod, D. (2019) Seasonal forecasts of the East African long rains: insight from atmospheric relaxation experiments. *Climate Dynamics*, 53, 4505–4520. <https://doi.org/10.1007/s00382-019-04800-6>.
- Maidment, R., Allan, R.P. and Black, E. (2015) Recent observed and simulated changes in precipitation over Africa. *Geophysical Research Letters*, 42, 8155–8164.
- McSweeney, C.F., Jones, R.G., Lee, R.W. and Rowell, D.P. (2015) Selecting CMIP5 GCMs for downscaling over multiple regions. *Climate Dynamics*, 44, 3237–3260.
- Munday, C. and Washington, R. (2018) Systematic climate model rainfall biases over Southern Africa: links to moisture circulation and topography. *Journal of Climate*, 31, 7533–7548.
- Mutai, C., Polzin, D. and Hastenrath, S. (2012) Diagnosing Kenya rainfall in boreal autumn: further exploration. *Journal of Climate*, 25, 4323–4329.
- Naiman, Z., Goodman, P.J., Krasting, J.P., Malyshev, S.L., Russell, J.L., Stouffer, R.J. and Wittenberg, A.T. (2017) Impact of mountains on tropical circulation in two Earth system models. *Journal of Climate*, 30, 4149–4163.
- Neupane, N. (2016) The Congo basin zonal overturning circulation. *Advances in Atmospheric Sciences*, 33, 767–782.
- Nicholson, S.E. (2015) Long-term variability of the East African ‘short rains’ and its links to large-scale factors. *International Journal of Climatology*, 35, 3979–3990.
- Nicholson, S.E. (2016a) An analysis of recent rainfall conditions in eastern Africa. *International Journal of Climatology*, 36, 526–532.
- Nicholson, S.E. (2016b) The Turkana low-level jet: mean climatology and association with regional aridity. *International Journal of Climatology*, 36, 2598–2614.
- Nicholson, S.E. (2017) Climate and climatic variability of rainfall over eastern Africa. *Reviews of Geophysics*, 55, 590–635.
- Nicholson, S.E. (2018) The ITCZ and the seasonal cycle over equatorial Africa. *Bulletin of the American Meteorological Society*, 99, 337–348.
- Ongoma, V., Chen, H. and Gao, C. (2017) Projected changes in mean rainfall and temperature over East Africa based on CMIP5 models. *International Journal of Climatology*, 38, 1375–1392.
- Rowell, D.P., Booth, B.B.B., Nicholson, S.E. and Good, P. (2015) Reconciling past and future rainfall trends over East Africa. *Journal of Climate*, 28, 9768–9788.
- Sanderson, B.M. and Knutti, R. (2012) On the interpretation of constrained climate model ensembles. *Geophysical Research Letters*, 39, L16708.

- Sanford, T., Frumhoff, P.C., Luers, A. and Gullede, J. (2014) The climate policy narrative for a dangerously warming world. *Nature Climate Change*, 4, 164–166.
- Schwendike, J., Govekar, P., Reeder, M.J., Wardle, R., Berry, G.J. and Jakob, C. (2014) Local partitioning of the overturning circulation in the Tropics and the connection to the Hadley and Walker circulations. *Journal of Geophysical Research – Atmospheres*, 119, 1322–1339.
- Shongwe, M.E., van Oldenborgh, G.J., van den Hurk, B. and van Aalst, M. (2011) Projected changes in mean and extreme precipitation in Africa under global warming. Part II: East Africa. *Journal of Climate*, 24, 3718–3733.
- Slingo, J., Spencer, H., Hoskins, B., Berrisford, P. and Black, E. (2005) The meteorology of the Western Indian Ocean, and the influence of the East African highlands. *Philosophical Transactions of the Royal Society A*, 363, 25–42.
- Stratton, R.A., Senior, C.A., Vosper, S.B., Folwell, S.S., Boutle, I.A., Earnshaw, P.D., Kendon, E., Lock, A.P., Malcolm, A., Manners, J., Morcrette, C.J., Short, C., Stirling, A.J., Taylor, C. M., Tucker, S., Webster, S. and Wilkinson, J.M. (2018) A pan-African convection-permitting regional climate simulation with the met office unified model: CP4-Africa. *Journal of Climate*, 31, 3485–3508.
- Tanaka, H.L., Ishizaki, N. and Kitoh, A. (2004) Trend and inter-annual variability of Walker, monsoon and Hadley circulations defined by velocity potential in the upper troposphere. *Tellus A*, 56, 250–269.
- Taylor, K.E., Stouffer, R.J. and Meehl, G.A. (2012) An overview of CMIP5 and the experiment design, 2012. *Bulletin of the American Meteorological Society*, 93, 485–498.
- Thalheimer, L. and Webersik, C. (2020) Climate change, conflicts and migration. In: Krieger, T., Panke, D. and Pregering, M. (Eds.) *Environmental Conflicts, Migration and Governance*. Bristol: Bristol University Press, p. 59.
- Tierney, J., Ummenhofer, C.C. and deMenocal, P.B. (2015) Past and future rainfall in the Horn of Africa. *Science Advances*, 1, e1500682.
- Uhe, P., Philip, S., Kew, S., Shah, K., Kimutai, J., Mwangi, E., van Oldenborgh, G.J., Singh, R., Arrighi, J., Jjemba, E., Cullen, H. and Otto, F. (2018) Attributing drivers of the 2016 Kenyan drought. *International Journal of Climatology*, 38, e554–e568.
- Vellinga, M. and Milton, S.F. (2018) Drivers of interannual variability of the East African long rains. *Quarterly Journal of the Royal Meteorological Society*, 144, 861–876.
- Vigaud, N., Lyon, B. and Giannini, A. (2017) Sub-seasonal teleconnections between convection over the Indian Ocean, the East African long rains and tropical Pacific surface temperatures. *International Journal of Climatology*, 37, 1167–1180.
- Viste, E. and Sorteberg, A. (2013) Moisture transport into the Ethiopian highlands. *International Journal of Climatology*, 33, 249–263.
- Wainwright, C.M., Marsham, J.H., Keane, R.J., Rowell, D.P., Finney, D.L., Black, E. and Allan, R.P. (2019) ‘Eastern African Paradox’ rainfall decline due to shorter not less intense short rains. *npj Climate and Atmospheric Science*, 2, 34. <https://doi.org/10.1038/s41612-019-0091-7>.
- Walker, D.P., Birch, C.E., Marsham, J.H., Scaife, A.A., Graham, R.J. and Segele, Z.T. (2019) Skill of dynamical and GHACOF consensus seasonal forecasts of East African rainfall. *Climate Dynamics*, 53, 4911–4935. <https://doi.org/10.1007/s00382-019-04835-9>.
- Washington, R., Harrison, H., Conway, D., Black, E., Challinor, A., Grimes, D., Jones, R., Morse, A., Kay, G. and Todd, M. (2006) African climate change: taking the shorter route. *Bulletin of the American Meteorological Society*, 87, 1355–1366.
- Washington, R., James, R., Pearce, H., Pokam, W.M. and Moufouma-Okia, W. (2013) Congo Basin rainfall climatology: can we believe the climate models? *Philosophical Transactions of the Royal Society B*, 368, 20120296.
- Williams, A.P. and Funk, C. (2011) A westwards extension of the warm pool leads to a westward extension of the Walker circulation, drying eastern Africa. *Climate Dynamics*, 37, 2417–2435.
- Yang, W., Seager, R., Cane, M.A. and Lyon, B. (2014) The East African long rains in observations and models. *Journal of Climate*, 27, 7185–7202.
- Yang, W., Seager, R., Cane, M.A. and Lyon, B. (2015a) The annual cycle of East African precipitation. *Journal of Climate*, 28, 2385–2404.
- Yang, W., Seager, R., Cane, M.A. and Lyon, B. (2015b) The rainfall annual cycle bias over East Africa in CMIP5 coupled climate models. *Journal of Climate*, 28, 9789–9802.
- Zaitchik, B. (2017) Madden-Julian Oscillation impacts on tropical African precipitation. *Atmospheric Research*, 184, 88–102.

How to cite this article: King JA, Washington R, Engelstaedter S. Representation of the Indian Ocean Walker circulation in climate models and links to Kenyan rainfall. *Int J Climatol*. 2021;41 (Suppl. 1):E616–E643. <https://doi.org/10.1002/joc.6714>